Fractional Josephson vortices at phase discontinuities

Habilitationsschrift

Dr. Edward Goldobin

Mathematisch-Naturwissenschaftliche Fakultät
Eberhard Karls Universität Tübingen

June 18, 2012

EBERHARD KARLS
UNIVERSITÄT
TÜBINGEN

Abstract

Quantization of magnetic flux in a superconducting loop is a cornerstone effect in the theory of superconductivity. In Josephson junctions this leads to the existence of the Josephson vortices carrying one quantum Φ_0 of magnetic flux. These vortices are called fluxons. By using π Josephson junctions or creating discontinuities of the phase artificially, we are able to create and study Josephson *semifluxons* or even arbitrary *fractional* Josephson vortices.

In this work I introduce and review π, 0-π and 0-κ Josephson junctions, where such vortices appear, and present technological developments of the last decade as well as experimental issues. By using 0-π Josephson junctions one can construct a φ junction, which can be used either as an eternal phase battery providing the phase $0 < \varphi < \pi$ to a superconducting circuit or as Josephson junction with magnetic field tunable current-phase relation. Further, I present the physics of fractional Josephson vortices, which is *very* different from the physics of integer vortices, namely, the ground states of a single vortex and of various vortex molecules; reconfiguration of fractional vortex molecules by using an external current; readout of vortex molecule states; the oscillatory modes of a single fractional vortex and of vortex molecules and crystals. Finally, in spite of rather large size of $\sim 100\,\mu$m, the fractional vortices exhibit macroscopic quantum effects — they can tunnel quantum mechanically and are predicted to allow a quantum mechanical superposition of the vortex and the antivortex.

Contents

Preface

After defending my Ph.D. degree in Moscow in 1997, my research activity was concentrated along several main directions related to the physics of Josephson junctions (JJs):

1. **Fluxon dynamics in stacked JJs**. Stacks of coupled long Josephson junctions (LJJs) have attracted a lot of attention in the mid 1990s because of the discovery of the intrinsic Josephson effect [KSKM92, KM94] and a possibility to build a stack of coherently operating (sub)-THz oscillators. The investigation of stacked LJJ was the main topic of my Ph.D. dissertation [Gol97]. After defending the Ph.D. degree this research lead to several interesting results. One of my main contributions is the discovery of the Cherenkov radiation by a fast moving Josephson vortex [GWTU98, GWU00, UGH+99] and the investigation of associated effects [KYG+99], *e.g.*, bunching of fluxons by means of Cherenkov radiation [GMU00]. Another important work is the experimental demonstration and explanation of "current locking" within the inductive coupling model [GU99]. I also observed in-phase zero-field steps [GNKU98], coupling of two LJJs in various modes [GU00], and other effects. Since I am not active in this field, I will not mention this activity below.

2. **Josephson ratchets**. Advantages of Josephson junction based ratchets are that: (I) directed motion results in an average dc voltage which is easily detected experimentally; (II) Josephson junctions are very fast devices which can operate (capture and rectify noise) in a broad frequency range from dc to $\sim 100\,\mathrm{GHz}$, capturing a lot of spectral energy; (III) by varying junction design and bath temperature both overdamped and underdamped regimes are accessible; and (IV) one can operate Josephson ratchets in the quantum regime.

   Focusing on Josephson vortex (fluxon) ratchets, we proposed several techniques to create an asymmetric periodic potential in a long Josephson junction [GSK01]: by LJJ width modulation, by bending the LJJ and by injecting auxiliary current with zero spatial average. The last technique proved to be very successful and we recently have demonstrated Josephson vortex (fluxon) ratchets with record figures of merit [BGN+05, KIS+12].

   This field is still of great interest as there are many questions to be investigated. For example, can one rectify (almost) white noise, i.e., a white noise with a cut off frequency? Although I am active in this field, I will not focus on this results in this habilitation.

3. **Anomalous proximity effect in High-T_c superconductors**. During my time with Oxxel GmbH we have made an important contribution to the clarification of a controversial issue of "giant/anomalous proximity effect" in cuprate superconductors. This became possible because of the atomically smooth interfaces that we were able to make using our Molecular Beam Epitaxy (MBE) machine [BLV+03, BLV+04]. Since I am not active in this field, I will not mention this activity below.

4. **Fractional flux quanta**. My main activity during the last few years is experimental and theoretical investigation of fractional flux quanta, i.e., Josephson vortices that carry half, or even any arbitrary fraction, of the magnetic flux quantum Φ_0. This is the main topic of this habilitation.

This habilitation is written in cumulative form, *i.e.*, it consists of an overview of the main results obtained by me and a set of relevant publications, submitted as habilitation thesis and attached at the end.

There are two lists of references in this work. First, it is the list of papers that constitute this habilitation. They are referenced using arabic numbers and listed in the section "Publications brought to habilitation" starting from the page 9. All other references (including my works not related to this habilitation) use author-year notation. The list starts on page 55.

This text is organized as follows. On page 7 a short summary of the work is given. The list of the works that constitute this habilitation can be found on page 9 followed by the discussion of my contribution on page 11 and of my group on page 12. In chapter 1 the basics, such as introduction to π and 0-π Josephson junctions, π SQUIDs are presented. Some of my works are references here already. The core of the work, presented in chapter 2, discusses the physics of fractional vortices: ground states in different systems, preparation and read-out of states, eigenmodes, dynamics, and finally macroscopic quantum effects. The main body of my works is cited here. In the text I focus on the concepts and give only some examples from experiments. Chapter 3 concludes the work. It presents the current status of research, unsolved problems and outlines the perspectives. Finally, at the end of this work one finds all my papers relevant to this habilitation attached.

Introduction

Since its discovery in 1911 superconductivity proved to be an exciting field of scientific research linking advances in material science with new concepts in quantum physics. The number of Nobel prizes[1] given in the field of superconductivity is probably larger than in any other field. Nowadays superconducting systems are routinely used in a broad spectrum of applications ranging from medicine to space research. New superconducting materials with unusual properties are still being discovered. In spite of numerous advances, the mechanism of superconductivity in some materials in not fully understood and active research in this field delivers some amazing results (e.g. π Josephson junctions). Since the beginning of the century investigation of controllable macroscopic quantum systems based on superconductors and their coherent interaction e.g. with light is at the forefront of research.

Superconductivity itself is a macroscopic quantum phenomenon. The existence of macroscopic wave function $\Psi(\boldsymbol{r})$, which describes coherent behavior of *all* electrons in the superconducting sample, is a fact of vital importance. As any complex function it can be written in general form as

$$\Psi(\boldsymbol{r}) = |\Psi(\boldsymbol{r})|e^{i\theta(\boldsymbol{r})},$$

where $\theta(\boldsymbol{r})$ is a phase. It is clear that $\Psi(\boldsymbol{r})$ and other derived quantities are 2π periodic functions of $\theta(\boldsymbol{r})$. In complex, not single connected geometries, *e.g.*, in a superconducting loop or hole, the phase may advance from $\theta(\boldsymbol{r}_0)$ to $\theta(\boldsymbol{r}_0)+2\pi n$, where n is integer, as one goes around the loop and arrives to the starting point $\boldsymbol{r}_0$. Note, there is no discontinuity of $\Psi(\boldsymbol{r})$, *i.e.*, of physical properties, anywhere. This advance of the phase by $2\pi n$ results in a *quantization of magnetic flux* $\Phi = n\Phi_0$ with the flux quantum $\Phi_0 = h/2e \approx 2.07 \times 10^{-15}$ Wb, which is a combination of fundamental constants: h is the Plank constant and e is the electron charge. Qualitatively, one can have the following picture in mind. The gradient of $\theta(\boldsymbol{r})$ induces the current in the loop, which generates magnetic field with total flux $\Phi = n\Phi_0$ threading the loop. Abrikosov vortices of supercurrent[2] existing in type-II superconductors also carry one flux quantum. Each vortex is essentially the superconducting loop around the tiny normal region. After discovery of Josephson effect[3] it turned out that Josepshon vortices existing in long Josephson junctions also carry one flux quantum Φ_0.

The lowest energy of the superconducting loop described above is achieved when no flux is trapped $n = 0$ and circulating supercurrent is zero. One can also include one (or more) Josephson junctions in such a loop to obtain a Superconducting QUantum Interference Device (SQUID). If those Josephson junctions are conventional junctions with a phase drop $\phi = \theta_2 - \theta_1 = 0$ in the ground state (when no supercurrent flows through it), nothing special happens with the ground state of the loop. By using unconventional superconductors or superconductor-ferromagnet hybrid structures one can fabricate a Josephson junctions with a phase drop of π in the ground state. So, if one instead uses the loop with one (or odd number of) such π junctions, the loop is frustrated – to provide a total phase advance of 0 or 2π around the loop the supercurrent *must* flow around the loop clockwise or counterclockwise. Since the total phase difference created by this current is only $\pm\pi$ — twice smaller by absolute value than in a loop without π JJ — the magnetic flux generated

[1] See Nobel Prizes 1913, 1962, 1972, 1973, 1987, 2003 at http://www.nobelprize.org

[2] Nobel prize 2003 given to Alexei A. Abrikosov, Vitaly L. Ginzburg, Anthony J. Leggett

[3] Nobel prize given in 1973 to L. Esaki, I. Giaever and B. D. Josephson

by this current in the loop is equal to $\pm\Phi_0/2$ — a half flux quantum.

Similar to the case of Josephson vortices carrying one flux quantum $\pm\Phi_0$ (fluxons) in long Josephson junctions, one can create and make experiments with Josephson *semifluxons* in long Josephson junctions consisting of 0 and π segments. Today we are even able to create not only semifluxons, but the vortices that carry an *arbitrary fraction* of the flux quantum Φ_0, *i.e.*, they are not quantized at all.

Such *fractional vortices* are very interesting objects and behave *very differently* from well known fluxons. This Habilitation summarizes my research on fractional vortex physics and also gives a reasonable overview of the works done by other groups. During one decade since the experimental discovery of semifluxons and later on of fractional vortices, their classical nonlinear physics is well understood. We are now able to create, manipulate, and readout the states of single vortices and molecules consisting of several fractional vortices; excite eigenmodes and make spectroscopy. The very latest achievement is that those unquantized fractional vortices nevertheless show a macroscopic quantum behavior. In particular, we observed a macroscopic quantum tunneling of a fractional vortex through a pinning barrier — quite an impressive result for an object that is $\sim 100\,\mu$m long.

Publications brought to Habilitation

[1] E. Goldobin, D. Koelle, and R. Kleiner. Semifluxons in long Josephson 0-π-junctions. *Phys. Rev. B*, 66:100508(R), 2002.

[2] E. Goldobin, D. Koelle, and R. Kleiner. Ground state and bias current induced rearrangement of semifluxons in 0-π-Josephson junctions. *Phys. Rev. B*, 67:224515, 2003.

[3] A. Zenchuk and E. Goldobin. Analytical analysis of ground states of 0-π long Josephson junctions. *Phys. Rev. B*, 69:024515, 2004.

[4] E. Goldobin, A. Sterck, T. Gaber, D. Koelle, and R. Kleiner. Dynamics of semifluxons in Nb long Josephson 0-π junctions. *Phys. Rev. Lett.*, 92:057005, 2004.

[5] T. Gaber, E. Goldobin, A. Sterck, R. Kleiner, D. Koelle, M. Siegel, and M. Neuhaus. Nonideal artificial phase discontinuity in long Josephson 0-κ junctions. *Phys. Rev. B*, 72(5):054522, 2005.

[6] E. Goldobin, N. Stefanakis, D. Koelle, and R. Kleiner. Fluxon-semifluxon interaction in an annular long Josephson 0-π junction. *Phys. Rev. B*, 70(9):094520, 2004.

[7] M. Weides, M. Kemmler, E. Goldobin, D. Koelle, R. Kleiner, H. Kohlstedt, and A. Buzdin. High quality ferromagnetic 0 and π Josephson tunnel junctions. *Appl. Phys. Lett.*, 89(12):122511, 2006.

[8] M. Weides, M. Kemmler, H. Kohlstedt, R. Waser, D. Koelle, R. Kleiner, and E. Goldobin. 0-π Josephson tunnel junctions with ferromagnetic barrier. *Phys. Rev. Lett.*, 97(24):247001, 2006.

[9] M. Weides, H. Kohlstedt, R. Waser, M. Kemmler, J. Pfeiffer, D. Koelle, R. Kleiner, and E. Goldobin. Ferromagnetic 0-π Josephson junctions. *Appl. Phys. A*, 89(3):613–617, 2007.

[10] J. Pfeiffer, M. Kemmler, D. Koelle, R. Kleiner, E. Goldobin, M. Weides, A. K. Feofanov, J. Lisenfeld, and A. V. Ustinov. Static and dynamic properties of 0, π, and 0-π ferromagnetic Josephson tunnel junctions. *Phys. Rev. B*, 77(21):214506, 2008.

[11] K. Buckenmaier, T. Gaber, M. Siegel, D. Koelle, R. Kleiner, and E. Goldobin. Spectroscopy of the fractional vortex eigenfrequency in a long Josephson 0-κ junction. *Phys. Rev. Lett.*, 98(11):117006, 2007.

[12] T. Gaber, K. Buckenmaier, D. Koelle, R. Kleiner, and E. Goldobin. Fractional Josephson vortices: oscillating macroscopic spins. *Appl. Phys. A*, 89(3):587–592, 2007.

[13] A. Dewes, T. Gaber, D. Koelle, R. Kleiner, and E. Goldobin. Semifluxon molecule under control. *Phys. Rev. Lett.*, 101(24):247001, 2008.

[14] U. Kienzle, T. Gaber, K. Buckenmaier, K. Ilin, M. Siegel, D. Koelle, R. Kleiner, and E. Goldobin. Thermal escape of fractional vortices in long Josephson junctions. *Phys. Rev. B*, 80(1):014504, 2009.

[15] E. Goldobin, D. Koelle, and R. Kleiner. Ground states of one and two fractional vortices in long Josephson 0-κ junctions. *Phys. Rev. B*, 70(17):174519, 2004.

[16] E. Goldobin, H. Susanto, D. Koelle, R. Kleiner, and S. A. van Gils. Oscillatory eigenmodes and stability of one and two arbitrary fractional vortices in long Josephson 0-κ junctions. *Phys. Rev. B*, 71(10):104518, 2005.

[17] H. Susanto, E. Goldobin, D. Koelle, R. Kleiner, and S. A. van Gils. Controllable plasma energy bands in a one-dimensional crystal of fractional Josephson vortices. *Phys. Rev. B*, 71(17):174510, 2005.

[18] Ch. Gürlich, E. Goldobin, R. Straub, D. Doenitz, Ariando, H.-J. H. Smilde, H. Hilgenkamp, R. Kleiner, and D. Koelle. Imaging of order parameter induced π phase shifts in cuprate superconductors by low-temperature scanning electron microscopy. *Phys. Rev. Lett.*, 103(6):067011, 2009.

[19] C. Gürlich, S. Scharinger, M. Weides, H. Kohlstedt, R. G. Mints, E. Goldobin, D. Koelle, and R. Kleiner. Visualizing supercurrents in ferromagnetic Josephson junctions with various arrangements of 0 and π segments. *Phys. Rev. B*, 81(9):094502, Mar 2010.

[20] S. Scharinger, C. Gürlich, R. G. Mints, M. Weides, H. Kohlstedt, E. Goldobin, D. Koelle, and R. Kleiner. Interference patterns of multifacet $20 \times$ (0-π) Josephson junctions with ferromagnetic barrier. *Phys. Rev. B*, 81(17):174535, May 2010.

[21] E. Goldobin, K. Vogel, O. Crasser, R. Walser, W. P. Schleich, D. Koelle, and R. Kleiner. Quantum tunneling of semifluxons in a 0-π-0 long Josephson junction. *Phys. Rev. B*, 72(5):054527, 2005.

[22] K. Vogel, W. P. Schleich, T. Kato, D. Koelle, R. Kleiner, and E. Goldobin. Theory of fractional vortex escape in a long Josephson junction. *Phys. Rev. B*, 80(13):134515, 2009.

[23] E. Goldobin, D. Koelle, R. Kleiner, and A. Buzdin. Josephson junctions with second harmonic in the current-phase relation: Properties of φ junctions. *Phys. Rev. B*, 76(22):224523, 2007.

[24] E. Goldobin, D. Koelle, R. Kleiner, and R. G. Mints. Josephson junction with a magnetic-field tunable ground state. *Phys. Rev. Lett.*, 107:227001, Nov 2011.

[25] U. Kienzle, J. M. Meckbach, K. Buckenmaier, T. Gaber, H. Sickinger, Ch. Kaiser, K. Ilin, M. Siegel, D. Koelle, R. Kleiner, and E. Goldobin. Spectroscopy of a fractional Josephson vortex molecule. *Phys. Rev. B*, 85:014521, Jan 2012.

[26] M. Kemmler, M. Weides, M. Weiler, M. Opel, S. T. B. Goennenwein, A. S. Vasenko, A. A. Golubov, H. Kohlstedt, D. Koelle, R. Kleiner, and E. Goldobin. Magnetic interference patterns in 0-π superconductor/insulator/ferromagnet/superconductor Josephson junctions: Effects of asymmetry between 0 and π regions. *Phys. Rev. B*, 81(5):054522, Feb 2010.

[27] M. Weides, U. Peralagu, H. Kohlstedt, J. Pfeiffer, M. Kemmler, C. Gürlich, E. Goldobin, D. Koelle, and R. Kleiner. Critical current diffraction pattern of SIFS Josephson junctions with a step-like F-layer. *Supercond. Sci. Technol.*, 23(9):095007, 2010.

Description of my own contribution

The investigation of semifluxons was started by me in the work [1] were I derived analytically the shape of a semifluxon and wrote a numerical code to confirm the analytical formulas numerically. Further in the work [2] I extended the numerical simulation code and performed extensive numerical simulation of different (re)arrangements of semifluxons. In the work [3] I made the statement of the problem. Most of analytical derivations were done by A. Zenchuk, while I was checking analytical results numerically and wrote the manuscript.

In the experimental work [4] I designed the samples, measured them together with T. Gaber, evaluated the results and wrote a manuscript together with other co-authors. In the following publication [5] T. Gaber invested a great deal of time investigating experimentally and numerically the effect of the finite injector size. I suggested several ideas how the finite injector size can be taken into account and wrote some simple analytical formulas that describe limiting cases.

In the numerical work [6] I was making numerical simulations together with N. Stefanakis who for the first time noticed the difference in dynamics of fluxons and semifluxons and proposed to investigate their interaction.

Back in 2003 I suggested to fabricate π and 0-π SIFS LJJs with high critical current density using a step-like thickness of the F-layer. M. Weides started his Ph.D. in FZ-Jülich to pursue this goal. The idea was successfully realized in the works [7] (separate 0 and π JJs) and [8–10] (0-π JJs). The samples were fabricated by M. Weides, while the measurements were done by M. Kemmler, J. Pfeiffer and me. I was also participating in designing the samples, analyzing obtained results and writing the paper.

In experimental works [11–14] I proposed the idea of experiment, participated in the samples design, evaluated obtained data and participated in writing the manuscript. The measurements were done by K. Buckenmaier and T. Gaber [11,12]; U. Kienzle, K. Buckenmaier and T. Gaber [14] and A. Dewes [13].

In a series of three theoretical works devoted to *arbitrary fractional* vortices [15–17] I was making analytical calculations (together with H. Susanto in [16, 17]), extensive numerical simulations in [15, 16], analysis of the results and preparation of the manuscript.

In two experimental works [18,19] using Low Temperature Scanning Electron Microscop (LTSEM) the experiment was performed by Ch. Gürlich, S. Scharinger, D. Dönitz using the samples fabricated by M. Weides [18,19] and by Ariando and H.-J. Smilde [18]. I analyzed experimental results, participated in fine tuning of experimental setup, made numerical simulations and participated in preparation of the manuscript. In a related work [20] I, together with R. Mints and R. Kleiner, suggested a model which allows to interpret our experimental observations, proposed the ideas for the experiment and prepared the manuscript.

In two theoretical paper about quantum properties of fractional vortices [21, 22] I formulated the problem, K. Vogel and O. Crasser derived the analytical formulas following discussion with T. Kato. Then I made numerical estimations (analytics was not possible up to the final result) to obtain final results and participated in preparation of the manuscript.

Lately, in the theoretical papers [23, 24] I derived analytically and also checked numerically the behavior of fractional vortices in LJJs with a second harmonic in the current-phase relation (CPR). I also wrote the manuscript where I discussed the possibility to observe the second harmonic experimentally and tune the CPR (including the ground state) by the applied magnetic field.

Finally, in experimental paper [25] I proposed the idea of experiment, participated in the samples design, evaluated obtained data and participated in writing the manuscript. The measurements were done by U. Kienzle, K. Buckenmaier, T. Gaber and H. Sickinger. The samples were fabricated by J. M. Meckbach, Ch. Kaiser and K. Ilin.

My Subgroup

During the course of this habilitation I was working as Assistant in the group Prof. R. Kleiner and Prof. D. Kölle. My "semifluxon" subgroup benefited from the work of the following people.

- Tobias Gaber. Ph.D. student from 05.2003 to 03.2007; defended Ph.D. thesis "Dynamics of fractional vortices in long Josephson junctions"; later Post. Doc. in the group; since 02.2012 he is at Bosch AG, Reutlingen.
- Albert Sterck. Ph.D. student from 04.2001 to 11.2005. Participated in some activities of the group, e.g., in works [4, 5].
- Kai Buckenmaier. Diploma student from 12.2005 to 11.2006; Ph.D. student from 12.2006 to 06.2010; defended Ph.D. thesis "Activation energy of fractional vortices and spectroscopy of vortex molecules in long Josephson junctions"; now he is at UC Berkeley, USA.
- Matthias Kemmler. Ph.D. student from 06.2003 to 02.2008; participated in some activity related to fractional vortex physics [7–10, 26, 27]; now he is Post. Doc. at the chair of Prof. R. Kleiner and Prof. D. Kölle.
- Judith Pfeiffer. Ph.D. student from 09.2006 to 01.2010; defended Ph.D. thesis "Fractional vortices in Josephson tunnel junctions with a ferromagnetic interlayer"; Since 2010 she is at Bosch AG, Reutlingen.
- Christian Gürlich. Ph.D. student from 04.2006 to 05.2010; defended Ph.D. thesis "Imaging of the current distribution in Josephson junctions with 0 and π facets"; since then he is at Daimler AG, Sindelfingen, Germany.
- Andreas Dewes. Diploma student from 06.2007 to 02.2008; defended Diploma thesis "Dynamics of fractional and integral flux quanta in long Josephson junctions"; now he is at the Quantronics group, Saclay, France
- Uta Kienzle. Diploma student from 06.2007 to 06.2008; defended Diploma thesis "Thermal and resonant activation in long Josephson junctions"; Ph.D. student since 07.2008. Defense is expected in summer 2012.
- Sebastian Scharinger. Ph.D. student since 11.2008. Defense is expected in summer 2012.
- Hanna Sickinger. Diploma student 10.2008–10.2009; defended Diploma thesis "Measurement of the eigenfrequencies of fractional vortex molecules in annular long Josephson junctions"; Ph.D. student since 12.2009; defense is expected in fall 2012.
- Benjamin Neumeier. Diploma 05.2010–05.2011. Defended Diploma thesis "Superconducting phase quantum bits"; Ph.D. student since 07.2011; Ph.D. defense is expected in 2014.
- Markus Turad. Ph.D. student since 10.2007. Defense is expected in summer 2012.
- Georg Rudolf. Diploma Student from 04.2011. Defense is expected in spring 2012.

Chapter 1

Basics

The supercurrent I_s through a conventional Josephson junction (JJ) is given by

$$I_s = I_c \sin(\phi), \tag{1.1}$$

where ϕ is the phase difference of the superconducting wave functions of the two electrodes, i.e. the Josephson phase [Jos62]. The critical current I_c is the maximum supercurrent that can flow through the JJ. In experiment one usually applies some current through the JJ and the junction reacts by changing the Josephson phase. From the above formula it is clear that the phase $\phi = \arcsin(I/I_c)$, where I is the applied (super)current.

Already in the original paper of Josephson [Jos62] it was predicted that Eq. (1.1) is the *simplest* relation that links the (super)current and the Josephson phase. Generally speaking, a current-phase relation (CPR) may deviate from a simple sinusoidal form (1.1), e.g., can have second harmonic component $\sim \sin(2\phi)$, be linear $j_s \propto \phi$ or even may have a more unusual shape. The CPR for a given type of the Josephson junction can be derived using a microscopic theory. For the time being we restrict ourselves with the CPR given by Eq. (1.1).

Since the phase is 2π-periodic, i.e. ϕ and $\phi + 2\pi n$ are physically equivalent, without loosing generality, we restrict the discussion below to the interval $0 \leq \phi < 2\pi$.

When no current ($I = 0$) is passing through the JJ, the JJ is in the ground state, the superconducting condensate in both electrodes establish a coherence with the phase difference (Josephson phase) across the JJ equal to zero ($\phi = 0$). The attentive reader may notice, that according to Eq. (1.1) the phase can also be $\phi = \pi$, also resulting in no current through the JJ.

To understand which state is realized in practice, one should introduce the notion of a Josephson energy $U(\phi)$. The Josephson energy is a potential energy associated with the Josephson phase ϕ or with the supercurrent j_s flowing through the JJ. Similar to the case of an inductance which accumulates a magnetic energy when the current flows through it, a Josephson junction accumulates the Josephson energy when a supercurrent flows. In the general case, the Josephson energy is just an integral of the CPR

$$U(\phi) = \Phi_0 \int I_s(\phi)\, d\phi. \tag{1.2}$$

In the simplest case of a sinusoidal CPR (1.1), the Josephson energy is

$$U(\phi) = E_J(1 - \cos\phi), \tag{1.3}$$

where $E_J = I_c\Phi_0/2\pi$ defines the typical scale of the Josephson energy and an integration constant was chosen so that $U(0) = 0$ for convenience.

Using Eq. (1.3) one calculates that the state with $\phi = \pi$ has $U(\pi) = 2E_J$ and corresponds to the energy maximum and, therefore, is *unstable*. The state $\phi = 0$ corresponds to the Josephson energy minimum and *is* a stable ground state.

1.1 π Josephson junctions

In certain cases one may obtain a JJ where the critical current is negative ($I_c < 0$). In this case the first Josephson relation becomes

$$I_s = -|I_c| \sin(\phi) = |I_c| \sin(\phi + \pi) \tag{1.4}$$

with the Josephson energy

$$U(\phi) = \frac{\Phi_0 |I_c|}{2\pi}(1 + \cos\phi) = E_J(1 + \cos\phi). \tag{1.5}$$

Obviously, the ground state of such a JJ is $\phi = \pi$ and corresponds to the Josephson energy minimum, while the conventional state $\phi = 0$ is unstable and corresponds to the Josephson energy maximum. Such a JJ with $\phi = \pi$ in the ground state is called π *Josephson junction*.

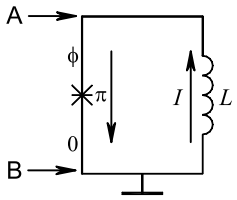

Figure 1.1: π JJ shorted by a superconducting wire (inductance). One can consider it as a single JJ SQUID (rf SQUID) with a π JJ.

A π JJ has quite unusual properties. For example, if one connects (shorts) the superconducting electrodes with an inductance L (e.g. superconducting wire), as shown in Fig. 1.1, one may expect a supercurrent circulating in the loop. Naively, recalling that the phase drop across the inductance is given by $\phi_L = LI \cdot 2\pi/\Phi_0$, the supercurrent is given by $I = \phi_L \Phi_0/(2\pi L) = \pi \cdot \Phi_0/(2\pi L)$. The reader may notice that for a very small inductance $L \to 0$, the supercurrent $I \to \infty$, which is unphysical. In fact, the current flowing through the inductance also flows through the π JJ. According to Eq. (1.4) this shifts the phase off from $\phi = \pi$, which decreases the current. The self-consistent calculations are given below.

Qualitatively, the supercurrent may indeed circulate if the inductance L is large enough. This state is degenerate, i.e. the current through the JJ and through the inductance can circulate clockwise or counterclockwise, corresponding to the initial phase (without inductive load) equal to $+\pi$ or $-\pi$. This supercurrent is spontaneous and belongs to the ground state of the system. It induces a magnetic field, which can be detected experimentally. The magnetic flux passing through the loop will have a value from 0 to a half of the magnetic flux quantum, i.e. from 0 to $\Phi_0/2$, depending on the value of inductance L.

Let us make a more detailed analysis of the circuit shown in Fig. 1.1. The current through the junction is given by

$$I = -|I_c| \sin\phi. \tag{1.6}$$

The Kirchhoff equation for the phases around the loop gives

$$\phi + \phi_L = \phi + LI\frac{2\pi}{\Phi_0} = 0, \tag{1.7}$$

where we assumed that there is no trapped flux in the loop.

These two Eqs. are for two unknowns I and ϕ. Excluding I we get the equation for the ground state phase ϕ:

$$\phi = \beta_L \sin(\phi), \tag{1.8}$$

where we introduced the "normalized" SQUID inductance

$$\beta_L = \frac{2\pi}{\Phi_0} L I_c. \tag{1.9}$$

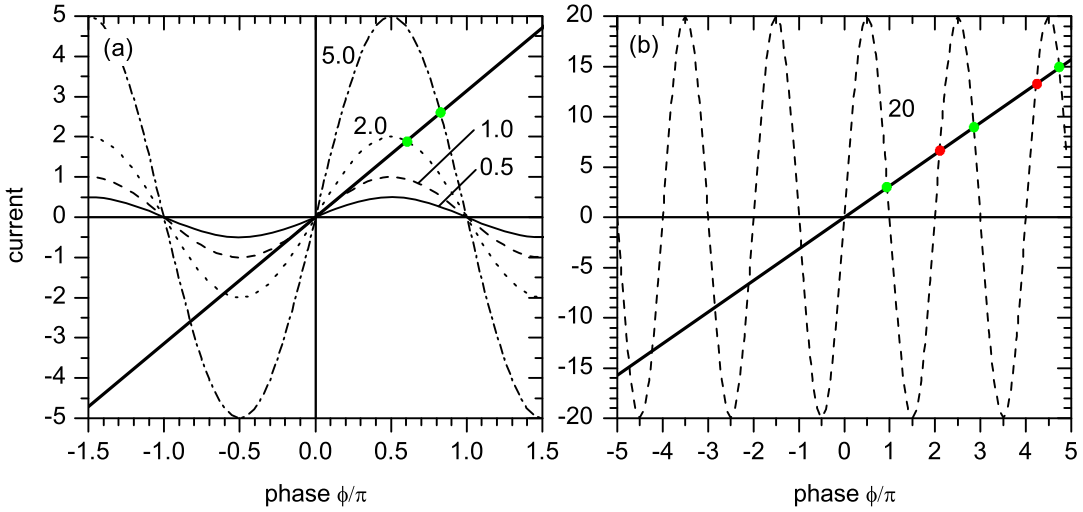

Figure 1.2: Graphical solution of Eq. (1.8). The l.h.s. is shown by straight solid line, the r.h.s. is shown as other line types for different values of β_L.

Equation (1.8) is a transcendental equation and cannon be solved analytically. Solving Eq. (1.8) graphically, as shown in Fig. 1.2, one sees that if $\beta_L < 1$ (small inductance) the only solution of (1.8) is $\phi = 0$. Therefore $I = 0$. When $\beta_L > 1$ a new non-trivial solution $\phi_0 \neq 0$ appears. It is shown in Fig. 1.2 by dots at the intersection of the $I = \phi$ line and the $I = \beta_L \sin(\phi)$ curve. One can notice that for $\beta_L \to \infty$, there are many intersections, i.e. many possible states of our single π JJ SQUID. In this limit ϕ_0 approaches π. For large β_L and not very large ϕ_0, i.e., $\pi(2n+1) - \phi_0 \ll \pi/2$, one can approximate the ground state solution as

$$\phi_0 \approx \pi(2n+1)\frac{\beta_L}{\beta_L + 1}. \tag{1.10}$$

One can also clarify the situation using energy arguments. The total energy of the π JJ SQUID is given by

$$E = E_L(I) + E_J(\phi) = \frac{LI^2}{2} + E_J\left(1 + \cos\phi\right), \tag{1.11}$$

where the sign $+$, instead of usual $-$, in front of the cos()-function says that we are dealing with a π JJ. Making use of Eq. (1.7), we express I and substitute it into Eq. (1.11). After trivial transformations we obtain

$$E(\phi) = E_J\left[\frac{\phi^2}{2\beta_L} + (1 + \cos\phi)\right]. \tag{1.12}$$

The plots of $E(\phi)$ for different values of β_L are shown in Fig. 1.3. For $\beta_L \leq 1$ there is only one energy minimum at $\phi = 0$, corresponding to the ground state of the system. At $\beta_L > 1$ the side minima appear, while the state $\phi = 0$ turns into an energy maximum. For very large β_L, see Fig. 1.3(b), there are several energy minima, situated close to the points $\phi = (2n+1)\pi$, see Eq. (1.10), but only $\phi_0 \approx \pm\pi$ is the true degenerate ground state of the π JJ SQUID.

Note that, to find all minima of the potential numerically one has to solve the problem $dE/d\phi = 0$ for ϕ, i.e. again the Eq. (1.8). Solving it, one will find a set of ϕ values corresponding to both the minima and the maxima of the potential, i.e. the stable and unstable solutions, as shown by

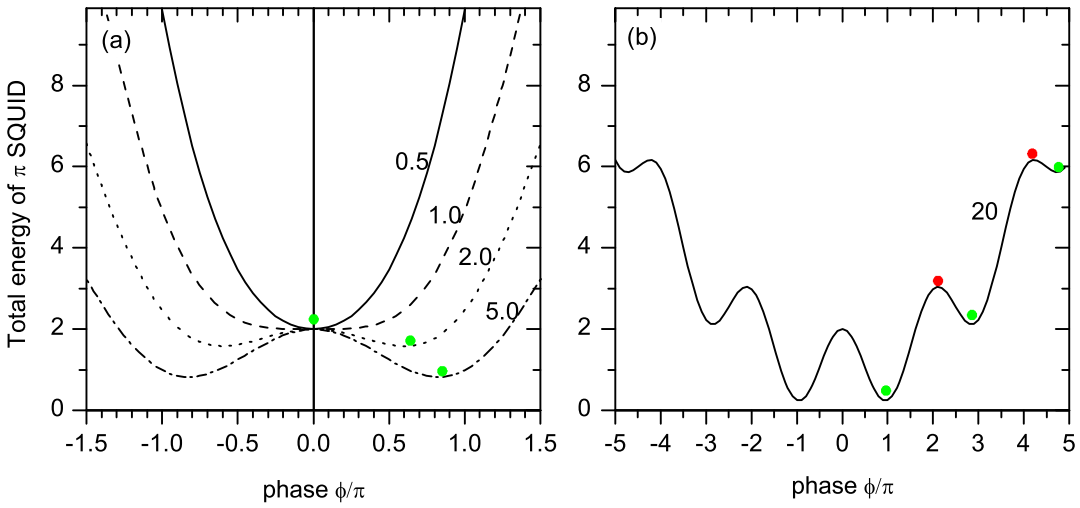

Figure 1.3: The plots of $E(\phi)$ for different values of β_L. (a) demonstrate the emergence of a ground state with $\phi_0 \neq 0$ for $\beta_L > 1$. (b) the behavior of energy at very large β_L.

the open and filled circles in Fig. 1.2 and 1.3. That is, each found solution should be checked for stability, e.g. for having $d^2E/d\phi^2 > 0$. This corresponds to the potential minimum and positive slope of $I_s(\phi)$ at the intersection points in Fig. 1.2.

Thus, a π JJ can be used as a "phase battery", pushing the supercurrent through the circuit connected to it. Similar to usual voltage batteries, the phase battery has finite loading capabilities. Given the inductance of the load L, the battery is able to supply supercurrent if its $|I_c| > \Phi_0/(2\pi L)$. If $|I_c| \gg \Phi_0/(2\pi L)$, then the battery will support a phase almost equal to π or some lower phase otherwise. *The phase battery does not discharge* as no energy is dissipated in the superconducting circuit in the regime described above.

1.1.1 Technologies and physical principles

Author's contributions: [7]

In Sec. 1.1 we have not mentioned *how* one can construct a π JJ. In fact, there are several physical effects that a π JJ can be based on.

1. **Tunnel JJ with spin flipping impurities in the barrier.** Consider a tunnel S|I|S Josephson junction with ferromagnetic impurities in I layer (ferromagnetic insulator). We denote such a JJ as S|FI|S. If one calculates the effect of spin flipping impurities on the Josephson tunneling supercurrent in the framework of the Anderson model [And61], one arrives to the result [Kul66] that

$$I_c \propto \frac{\langle|T_n|^2\rangle - \langle|T_s|^2\rangle}{\langle|T_n|^2\rangle + \langle|T_s|^2\rangle}, \tag{1.13}$$

where $\langle|T_s|^2\rangle$ and $\langle|T_n|^2\rangle$ are the angle averaged transmission probabilities with and without spin flipping, accordingly. It is obvious from Eq. (1.13) that I_c may become negative when the spin flipping tunneling dominates. This limit was not discussed in the original work [Kul66]. The word "π junction" first appeared in Ref. [BKS77] where the consequences of having a negative critical current due to Eq. (1.13) were analyzed for the first time. The first implementation of a S|FI|S π JJ was reported [VGG+06].

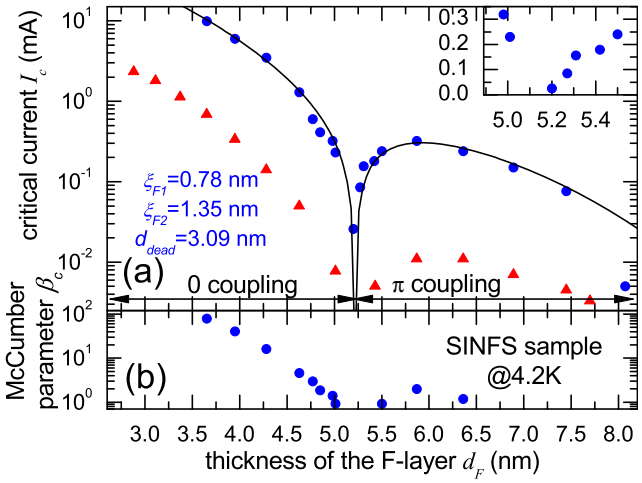

Figure 1.4: An example of experimental dependence $I_c(d_F)$ measured using a set of samples fabricated in the same technological run with a gradient in thickness d_F across the wafer. Adapted from Ref. [7].

Recently, there was also a proposal to use a "native" ferromagnetic insulator such as La_2BaCuO_5 as a Josephson barrier. In such a material the spin up and spin down conduction bands are completely separated so that one of them is 100% filled and the other is empty. The chemical potential lays in between the spin subbands, resulting in a 100% spin polarized insulator. Due to the specific energy band structure, the electrons tunneling from one superconductor to another through such a barrier experience a phase shift of π if they tunnel through an odd number of atomic layers (unit cells). [KAT+10]

2. **Ferromagnetic Josephson junctions**. Consider a Josephson junction with ferromagnetic Josephson barrier, *e.g.*, the multi-layer structures **S**uperconductor-**F**erromagnet-**S**uperconductor (S|F|S) or **S**uperconductor-**I**nsulator-**F**erromagnet-**S**uperconductor (S|I|F|S). In such structures the superconducting order parameter inside the F-layer oscillates in the direction perpendicular to the JJ plane. As a result, for certain thicknesses of the F-layer and temperatures, the order parameter may become $+1$ at one at one superconducting electrode and -1 at the other superconducting electrode. In this situation one gets a π Josephson junction. Note that inside the F-layer a competition of different solutions takes place and the one with the lower energy wins. Ferromagnetic π junction were fabricated by several groups:

   - S|F|S JJs [ROR+01, BTKP02, BBA+04];
   - S|I|F|S JJs [KAL+02] [7].

   As an example in Fig. 1.4 one can see the dependence $I_c(d_F)$ measured in our group experimentally.

3. **JJs with unconventional order parameter symmetry**. Novel superconductors, notably high temperature cuprate superconductors, have an anisotropic superconducting order parameter which can change its sign depending on the direction. In particular, the so-called d-wave order parameter has a value of $+1$ if one looks along the crystal axis a (or b) and -1 if one looks along the crystal axis b (or a). If one looks along the ab direction (45° between a and b) the order parameter vanishes. By making Josephson junctions between d-wave superconducting films with different orientation or between d-wave and conventional isotropic s-wave superconductor, one can get a phase shift of π. Nowadays there are several realizations and proposals of π JJs of this type:

   - tri-crystal grain boundary JJs [TK00];

- tetra-crystal grain boundary JJs [CSB+02, CEM+03];
- d-wave/s-wave ramp zigzag JJs [VH95, SAB+02, ADS+05, HAS+03];
- tilt-twist grain boundary JJs usually fabricated using biepitaxy [LTR+02, TKLG03, LJB+06, SRC+10];
- p-wave based JJs [GL86, GLB87];
- "geometric" π junctions [GIS07].

4. **Non-equilibrium Josephson junctions**. **S**uperconductor-**N**ormalMetal-**S**uperconductor (SNS) Josephson junctions with a nonequlibrium electron distribution in the N-layer, which can be created by the external current injection [BMWK99, HPH+02].

5. **Superconductor-QuantumDot-Superconductor JJ**. The operation of a Superconductor-QuantumDot-Superconductor (S|Q|S, S|QD|S, S•S) JJs is conceptually similar to the usual SIS JJs with the spin flipping ferromagnetic impurities in the I-barrier, but one speaks about one conduction channel only. As a quantum dot one usually uses a single wall carbon nanotube (SWCNT) or a semiconducting nanotube, both of which have only a single conduction channel. The flow of supercurrent through a S|CNT|S (CNT is proximized by S) was shown experimentally [KDK+99, JHvDK06, PGRS08]. A tunable supercurrent through the semiconducting nano-wire was demonstrated [DvDR+05]. The S|CNT|S JJs, tunable between the 0 and the π state by a gate voltage, were demonstrated [CWB+06, JNGR+07].

6. **A superfluid ^{3}He Josephson junction** may also be made such that it possesses a phase π in the ground state [MSB+99].

1.1.2 Historical developments

Theoretically, the possibility to have π JJs was discussed for the first time in 1977 by Bulaevskii et al. [BKS77], who considered a JJ with paramagnetic scattering in the barrier. Almost one decade later the possibility of having a π JJs was discussed in the context of heavy fermion p-wave superconductors [GL86, GLB87].

Experimentally, the first π JJ was a corner JJ made of YBCO (d-wave) and Pb (s-wave) superconductors [VH95]. The π JJs based on ferromagnetic barrier were first fabricated and investigated only a decade later [ROR+01].

1.2 Applications of π Josephson junctions

There is a number of proposals how π JJs can revolutionarize existing and contribute to emerging technologies. One obvious application is to use π JJs as a "phase battery", which will provide a phase close to π. In some circuits such phase batteries will allow to decrease the number (or completely get rid) of the bias lines. In quantum circuits, which should be decoupled from the environment, intrinsic bias may drastically reduce the decoherence figures. For many applications one has to use 0 and π JJs fabricated on the *same chip* during the *same technological run*. This can make the technology somewhat more complicated. For example, in the case of d-wave/s-wave ramp zigzag junctions, there are no such complications, but in case of S|F|S, S|I|F|S or S|FI|S technologies one has to add at least one additional technological step. Below we discuss several applications of π JJs in details.

- **Digital superconducting circuits** such as RSFQ [LS91], potentially have very high speed of operation (sub-THz clock frequencies) and very low power consumption in the JJ per switching event. The problem is that approximately every second JJ should be dc biased by a current of the order of the critical current of the junction. Usually, one employs a bias bus with voltage $V_{\rm bias}$, which is connected with all bias points through bias resistors. It turns

out that the power dissipated by these bias resistors is by several orders of magnitude larger than the power dissipated by the JJs during switching events. Thus, a reduction or removal of the bias lines is very desirable.

There were several proposals how to use π JJs in RSFQ circuits. These proposals can be conceptually separated into two categories: *active* π JJs and *passive* π JJs. Under active we mean π JJs that are (temporarily) switching to the voltage state during operation. Passive π JJs always stay in the superconducting state, i.e. they really work as a phase battery.

The use of *active* π JJs in RSFQ circuits was suggested and recently implemented [OAM+06] using a $YBa_2Cu_3O_7$-Nb (d-wave/s-wave) ramp zigzag 0-π JJs technology. A simple circuit consisting of a DC-to-SFQ converter, a Josephson transmission line, a T-flip-flop and a SFQ-to-DC converter had smaller number of bias lines, larger margins and allows for a symmetric design of the cells avoiding time consuming numerical optimization of the working point with maximum margins. Requirements to π JJs that are supposed to be used as active elements are the same as to 0 JJs: similar I_c, similar resistance R and similar characteristic voltage $V_c = I_c R$. V_c defines an upper limit for the operating frequency ($\sim \Phi_0 V_c$) of such RSFQ circuits. Among all π JJ technologies the d-wave/s-wave ramp zigzag technology and the S|I|F|S technology [8, 9] provide 0 and π JJs with similar parameters. Similar results can be, in principle, obtained using grain boundary JJs, but one usually can have only few (1,2,3) grain boundaries on each crystal, thus strongly limiting topologically the freedom of the circuit design.

In another approach π JJs are used as *passive* phase shifters [UK03,KBM+10,FOB+10]. This allows not only to self bias the circuit but also to use π JJs instead of geometric inductances, thus, drastically decreasing the geometrical sizes of every RSFQ cell. The only requirement for a π JJ used passively is that they should have a rather high critical current and do not switch into the resistive state during operation. The authors also claim that $I_c R_n$ should be similar to that of active JJs, so that the π shifter is able to follow the dynamics of the circuit and keep the phase difference even during fast changes of the phase. In terms of technology, the successful implementation of a qubit [FOB+10] and RSFQ T-flip-flop [KBM+10] based on SFS π JJ was reported.

- **Complementary circuits** similar to CMOS semiconducting circuits were proposed [TGB97, TB97, TB98]. The idea is that having complementary 0 and π JJs, one can build superconducting electronic circuits with symmetric layout and large margins. The main requirements here is to either have 0 and π JJs with the same parameters such as I_c, damping, *etc.* or use high I_c π JJs simply as phase shifters.

1.3 0-π Josephson junctions

The ground state of a 0 JJ is $\phi = 0$, while the ground state of π JJ corresponds to $\phi = \pi$. What will happen if one connects two such junctions in parallel, as shown in Fig. 1.5? In particular, what will be the ground state of such a system? Let us consider two cases depicted in Fig. 1.5a and b.

1.3.1 0-π dc SQUID

The first case, shown in Fig. 1.5a, corresponds to two point-like JJs in a loop with inductance L. This is nothing else as a two JJ SQUID (aka dc SQUID) where one of the JJs is a π JJ.

The potential energy of such a π dc SQUID can be written as

$$U = -\cos(\mu_0) - R_I \cos(\mu_\pi) + \frac{1}{2\beta_{L0}} \left[\mu_0 - \mu_\pi + 2\pi f\right], \tag{1.14}$$

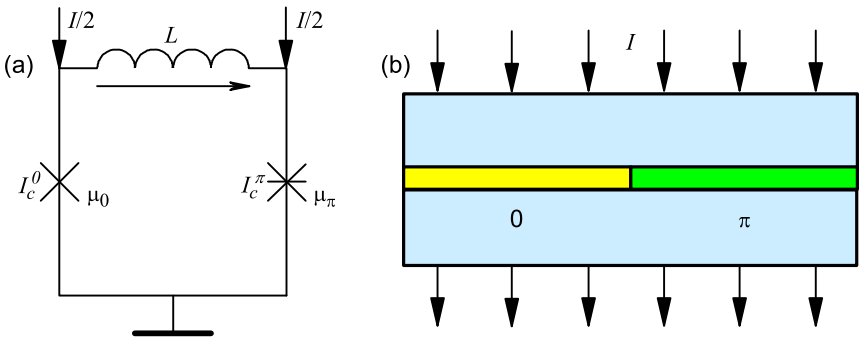

Figure 1.5: Two qualitatively similar systems: (a) a π dc SQUID with one 0 JJ and one π JJ and (b) a 0-π JJ. A 0-π JJ (b) can be considered as a π dc SQUID with zero loop area and extended (long), rather than point-like, JJs.

where U is normalized to the Josephson energy of the 0 JJ, $E_{J0} = I_{c0}\Phi_0/2\pi$. The SQUID parameter $\beta_{L0} = 2\pi I_{c0}L/\Phi_0$. The parameter $R_I = I_{c\pi}/I_{c0}$ ($|R_I| \leq 1$) describes the ratio of critical currents (while $|R_I|$ describes the ratio of Josephson energies). The parameter f in Eq. (1.14) is a frustration (normalized applied magnetic field). Note that the phases μ_0 and μ_π are not independent. They are linked by the common current that flows through both junctions (the bias current is assumed to be zero). For $|R_I| \leq 1$ the good phase variable turns out to be μ_π, so that μ_0 can be expressed as

$$\mu_{01} = -\arcsin[R_I \sin(\mu_\pi)]; \tag{1.15}$$

$$\mu_{02} = +\arcsin[R_I \sin(\mu_\pi)] - \pi. \tag{1.16}$$

For further discussion, only μ_{01} is relevant and corresponds to the ground state of the system. To study the ground state, we further assume $f = 0$ and focus, first, on the simplest case $R_I = -1$. The plots $U(\mu_\pi)$ for different values of β_{L0} are shown in Fig. 1.6.

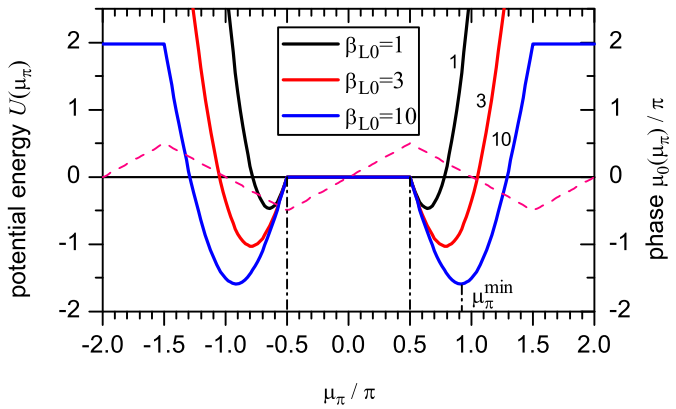

Figure 1.6: The energy of the π dc SQUID as a function of μ_π. The values of the phase $\mu_{01}(\mu_\pi)$ (1.15) are shown as well.

One can see that for $|\mu_\pi| < +\pi/2$, the energy $U(\mu_\pi)$ is constant, $\mu_{01} = \mu_\pi$, so that no currents are circulating. For $|\mu_\pi| > +\pi/2$ an energy minimum is visible. Its position $\mu_\pi^{\min}$ and depth $U(\mu_\pi^{\min})$ depends on β_{L0}. As one can see, the phases of the JJs are not equal, which corresponds to a spontaneous supercurrent which circulates in the SQUID loop. For minima at $\pm\mu_\pi^{\min}$ this

supercurrent has opposite directions (clockwise or counterclockwise). It also produces spontaneous magnetic flux, which is equal to

$$\Phi = \frac{\Phi_0}{2\pi}[\mu_{01}(\mu_\pi^{\min}) - \mu_\pi^{\min}] = \frac{\Phi_0}{2\pi}[\pi - 2\mu_\pi^{\min}], \tag{1.17}$$

where we took into account that in the region $\mu_\pi > \pi/2$, $\mu_{01} = \pi - \mu_\pi$, *cf.*, Eq. (1.15). To find the value of $\mu_\pi^{\min}$ for given β_{L0} one has to solve the following transcendental equation

$$\beta_{L0} \sin \mu_\pi = 2\mu_\pi - \pi, \tag{1.18}$$

for μ_π. The result is presented in Fig. 1.7(a) together with two analytical approximations

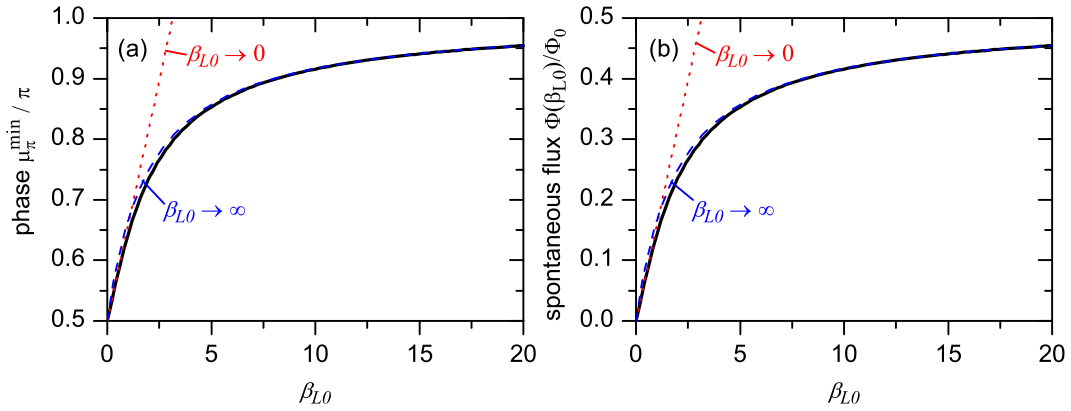

Figure 1.7: (a) The solution of the transcendental Eq. (1.18) $\mu_\pi^{\min}(\beta_{L0})$ (solid line) together with two approximations given by Eqs. (1.19) (dotted line) and (1.20) (dashed line). (b) The value of spontaneous flux $\Phi(\beta_{L0})$ (solid line) as well as analytical approximations given by Eqs. (1.21) (dotted line) and (1.22) (dashed line).

$$\mu_\pi^{\min} \approx \frac{\pi + \beta_{L0}}{2}, \quad \beta_{L0} \ll 1; \tag{1.19}$$

$$\mu_\pi^{\min} \approx \pi\frac{\beta_{L0} + 1}{\beta_{L0} + 2}, \quad \beta_{L0} \gg 1. \tag{1.20}$$

As one can see, Eq. (1.20) describes the behavior of $\mu_\pi^{\min}(\beta_{L0})$ rather accurately in the whole range of β_{L0} and even gives the right value at $\beta_{L0} = 0$.

The values of spontaneous flux $\Phi(\beta_{L0})$ calculated from $\mu_\pi^{\min}(\beta_{L0})$ using Eq. (1.17) are shown in Fig. 1.7(b). The corresponding approximations

$$\Phi = \pm\frac{\Phi_0}{2\pi}\beta_{L0}, \quad \beta_{L0} \ll 1; \tag{1.21}$$

$$\Phi = \pm\frac{\Phi_0}{2\pi}\frac{\pi\beta_{L0}}{\beta_{L0} + 2}, \quad \beta_{L0} \gg 1, \tag{1.22}$$

are also shown in Fig. 1.7(b). One can see that in the case of a perfectly symmetric π dc SQUID the ground state is degenerate and corresponds to a spontaneously circulating supercurrent inducing a spontaneous magnetic flux with the value between 0 and $\Phi_0/2$ depending on inductance of the SQUID β_{L0}. Note, that in contrast to a π SQUID with a *single* JJ, considered in the Sec. 1.1, the circulating supercurrents are always flowing regardless of the value of inductance.

1.3.2 0-π long Josephson junctions

Fig. 1.5b shows the so-called 0-π long Josephson junction (LJJ). It is a LJJ which consists of different parts having the properties of 0 and of π JJs, if taken separately.

Below, we use the name 0-π LJJ (a) to speak, in general, about a LJJ with several 0 and π parts and (b) to denote the particular case shown in Fig. 1.5b. When necessary we will use notations like 0-π-0 LJJ or 0-π-0-π LJJ, but in general all such junctions will be called 0-π LJJs.

It is clear that the two parts of the structure shown in Fig. 1.5b should somehow agree what will be the ground state of the whole system. It turns out that if the JJ is long enough, the phase far in the 0 region will be zero. Far in the π region it will be π, and it will change smoothly between 0 and π in the vicinity of the 0-π boundary, as shown in Fig. 2.3a. Such a spatial variation of the phase in the ground state implies the presence of the local magnetic field $B \propto \mathrm{d}\,\mu(x)/\mathrm{d}\,x$, *i.e.*, localized in the vicinity of the 0-π boundary. The total flux associated with this magnetic field is equal to the *half* of the magnetic flux quantum $\Phi_0 \approx 2.07 \times 10^{-15}$ Wb. Such a *semifluxon* is pinned at the 0-π boundary and corresponds to the ground state of the system. Further, if one looks at the Josephson supercurrent distribution in the vicinity of the 0-π boundary ($\propto j_c(x) \sin\phi$), one finds that the Josephson current flows in different directions in these 0 and π parts. Since we are investigating the ground state and do not supply any external bias, this currents should close somehow. In fact, they form a vortex of supercurrent circulating around the 0-π boundary in the clockwise direction, as shown on the sketch in Fig. 1.5.

In principle the $+\pi$ and $-\pi$ ground states of the π part are equivalent because the phase is defined mod2π. However, in 0-π LJJ this makes an important difference. If the phase changes along the LJJ not from 0 to $+\pi$, but from 0 to $-\pi$, then the one gets an *antisemifluxon*, carrying the flux $-\Phi_0/2$, and having the supercurrent circulating around 0-π boundary counterclockwise.

Thus, a semifluxon is a Josephson vortex pinned at the 0-π boundary. It forms the generate ground state of the system with two possible polarities of the magnetic flux $\pm\Phi_0/2$, corresponding to clockwise or counterclockwise circulation of the supercurrent around the 0-π boundary. In this sense, it resembles a classical spin or any other two-state system and we will often use spin notations $\uparrow$ and $\downarrow$ to denote two different polarities of the semifluxon.

1.3.3 0-π Josephson junction technologies

Author's contributions: [4, 8–10, 18, 19, 26, 27]

Some technologies that can be used to fabricate π JJs can also be used to fabricate 0-π LJJs, *e.g.*, SFS or SIFS technologies. However, there are technologies, *e.g.*, JJs based on d-wave superconductors, that allow only to fabricate 0 and π JJs, but not a π JJ alone. Other technologies, *e.g.*, non-equilibrium SNS or quantum dot based JJs, allow to fabricate single π JJs or, may be, 0-π SQUIDs or arrays, but do not allow to fabricate a continuous LJJ with uniform parameters. In principle, one could always fabricate a JJ array in the continuous limit (having small discreteness parameter, *i.e.*, the loop inductance), but then one should tune each of a few dozens of junctions separately, which seems not very feasible.

Below we present several technologies which, nowadays, are the most relevant for the fabrication of 0-π LJJs.

1. **JJs with unconventional order parameter symmetry**. Most of the technologies based on unconventional order parameter symmetry described in sec. 1.1.1 on p. 17, except "geometric" π junction, can be used to fabricate 0-π JJs. The physical principle is the same: due to d-wave order parameter symmetry, there is a π-phase shift between electrons with perpendicular momenta. The known technologies are:

   - tri-crystal grain boundary JJs [TK00];
   - d-wave/s-wave corner JJs [VH95] or ramp zigzag JJs [SAB+02, ADS+05, HAS+03] [18];

- $YBa_2Cu_3O_7$ grain boundary JJs fabricated using biepitaxy on CeO_2 as a seed layer [CBP+10, CKB+10];

Within this work images of supercurrent distribution in $YBa_2Cu_3O_7$-Nb and $Nd_{2-y}Ce_yCuO_x$-Nb ramp zigzag JJs were obtained using LTSEM [18]. These images clearly show a Josephson current counterflow in neighboring facets in zero magnetic field. The $I_c(H)$ dependence in such 0-π JJs is clearly not Fraunhofer-like, exhibiting main maxima at finite magnetic field and low $I_c(0)$ [18] [SAB+02, ADS+05].

2. **Ferromagnetic Josephson junctions**. The SFS or SIFS technology described in sec. 1.1.1 on p. 17 can also be used to fabricate 0-π LJJs. For this, one should vary the thickness of the ferromagnet barrier in a step-wise manner so that the parts with the thickness d_{F1} will correspond to a 0 JJ, while the parts with d_{F2} to a π JJ. Usually, one also would like to have almost equal critical currents of the 0 and π parts, which requires precise control of d_F on the level below 1 nm over both thicknesses. Such 0-π JJs were fabricated already by several groups:

   - SFS JJs [DRAK+05, FVHB+06] were, in fact, obtained by chance. The step in F-layer was formed because of misalignment during the fabrication process.
   - 0, π and 0-π JJs based on SIFS technology were fabricated intentionally [8,9] and show the best parameters among ferromagnetic 0-π JJs.
   - One can also use the S|FI|S technology [VGG+06], again with a step-like thickness of the FI layer, but this was not demonstrated yet.

   Within this work were able to fabricate the SIFS 0-π JJs of various (complicated) shapes: rectangular 0, π, 0-π, 0-π-0 and $20 \times (0\text{-}\pi)0$-$\pi$- JJs; annular 0-$\pi$ JJ' disk-shaped 0-π JJs. The Josephson current density in these devices was imaged using LTSEM at different applied magnetic fields and a good agreement with the theory was found [19].

   Since LTSEM measurements are very time-consuming, in practice, the fastest way to characterize just fabricated 0-π JJs is to measure their $I_c(H)$ dependence. When the magnetic field H is applied in the plane of the JJ *perpendicular* to the 0-π boundary (the step in F-layer) the $I_c(H)$ dependence is Fraunhofer-like, while, by applying the field H *along* the 0-π boundary, the $I_c(H)$ dependence has a minimum near $H = 0$ and two main maxima at finite field [10]. Also, it is very useful to have reference 0 (with $d_F = d_{F1}$) and π (with $d_F = d_{F2}$) JJs that are fabricated during the same run and have the same geometry as 0-π JJ. The comparison of $I_c(H)$ dependences of all three JJs allows to extract parameters just as critical densities $j_{c,0}$ and $j_{c,\pi}$ in 0 and π parts of 0-π JJ. As an example, in Fig. 1.8 the $I_c(H)$ dependences for 0, for π and for 0-π JJs are shown. In general, it is very difficult to fabricate SFS or SIFS 0-π JJ with $j_{c,0} = j_{c,\pi}$. Often one may change j_c's within some limits by changing the temperature, *cf.*, Fig. 1.8(a) and (b). In addition, the multi-domain F-layer may have different net remanent magnetization in 0 and π parts. The effects of these asymmetries on $I_c(H)$ dependence in SIFS 0-π JJs was studied by us in several works [26,27]

3. **Artificial 0-π Josephson junctions**. One can create a 0-π LJJ artificially using a pair of current injectors [4]. For this one can use the widely available Nb-AlO_x-Nb technology, which in addition provides a broad range of j_c and exponentially low damping at low temperatures so that one can even observe macroscopic quantum effects. The samples can be ordered from commercial suppliers such as Hypres. [Hyp]

4. **Phase shift created by an Abrikosov vortex situated close to the Josephson barrier**. If a single Abrikosov vortex is situated (pinned) close to the Josephson barrier and parallel to it, it will cause a phase gradient along the Josephson barrier. Since the total phase twist around the Abrikosov vortex is 2π, one can induce a phase difference of π or less along the Josephson barrier. The phase difference depends on the length of the LJJ and the distance between the Josephson barrier and the Abrikosov vortex. In the case when the

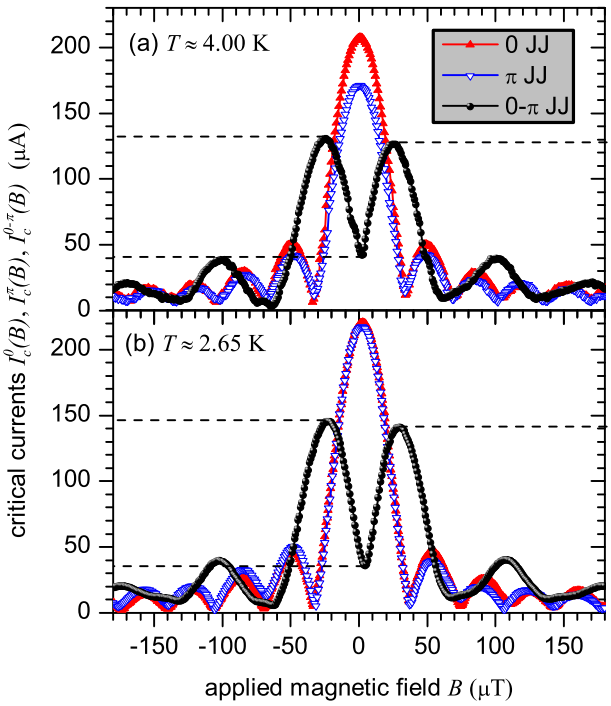

Figure 1.8: An example of $I_c(H)$ dependences for 0, for π and for 0-π JJ at two different temperatures. The $I_c(H)$ dependence for a 0-π JJ has a characteristic minimum near zero magnetic field H. One can also observe that the critical currents of the 0 and π facets can be made equal by varying the temperature. Adapted from Ref. [8]

Abrikosov vortex is pinned very close to the barrier, the phase difference is almost π and the Josephson phase changes from ϕ to $\phi + \pi$ in the λ_L-vicinity of the Abrikosov vortex, where λ_L is the London penetration depth. The original theoretical proposal [AG84] was realized only recently in nano-junctions, fabricated using FIB [GRK10].

1.3.4 Applications of 0-π Josephson junctions

In addition to applications discussed in Sec. 1.2 where single 0 and π JJs are needed, the 0-π JJs are used are used to investigate the order parameter symmetry in novel superconductors. For example, the d-wave order parameter in cuprate superconductors was established in a series of works on corner JJs [VH95], tri-crystals [TK00, KCK00, TK02, KTM99, KTR+96, SYI02], tetra-crystals [CSB+02, CEM+03], ramp [SAB+02, ADS+05, KTA+06] JJs.

The other application are based on spontaneously arising semifluxons. They will discussed in Sec. 2.7 after the discussion of the physics of fractional Josephson vortices.

Chapter 2

Physics of fractional vortices

2.1 Model

Author's contributions: [1, 4]

The model which describes the dynamics of the Josephson phase in 0-π LJJs was derived in different contexts. First, it was derived for a LJJ consisting of two parts: one with a dominant spin-flip Josephson tunneling resulting in $j_c < 0$, and another part with dominant normal tunneling with $j_c > 0$ [BKS78]. Then the same model was introduced to describe JJs based on d-wave superconductors [XMT95,KCK00,KBM95]. In comparison with the previous cases that considered some particular (mostly static) cases, we have derived the full dynamical perturbed sine-Gordon equation in the context of d-wave/s-wave LJJs [1]. The same equations were also derived to describe the pinning effect of an Abrikosov vortex on the fluxon dynamics in LJJ [AG84]. In any case, the perturbed sine-Gordon equation is the same for all types of LJJs, but it can be written in different forms.

In essence one can use two main approaches. First approach is natural when one starts from the fact that the critical current $j_c(x)$ is coordinate dependent. In this case, one can derive the following obvious generalization of the usual sine-Gordon equation

$$\mu_{xx} - \mu_{tt} - \tilde{j}_c(x)\sin(\mu) = \alpha\mu_t - \gamma(x). \tag{2.1}$$

Here the Josephson phase is denoted as $\mu(x,t)$ and $\tilde{j}_c(x) = j_c(x)/j_{c0}$ is the normalized critical current density which changes along the LJJ, $j_{c0} > 0$ is the "typical" current density. The coordinate x is normalized to the Josephson penetration depth

$$\lambda_J = \sqrt{\frac{\Phi_0}{2\pi\mu_0 d' j_{c0}}}, \tag{2.2}$$

where $\mu_0 d'$ is the inductance of a square of the superconducting films forming the JJ. The time t is normalized to the inverse plasma frequency $1/\omega_p$, where

$$\omega_p = \sqrt{\frac{2\pi j_c}{\Phi_0 c}}. \tag{2.3}$$

Here c is the specific capacitance between electrodes forming the JJ. The subscripts x and t in Eq. (2.1) denote the partial derivatives with respect to coordinate x and time t, the dimensionless damping coefficient $\alpha \equiv 1/\sqrt{\beta_c}$, and β_c is the McCumber-Stewart parameter [Lik86]. The function $j_c(x)/j_{c0}$ in the simplest case of a 0-π LJJ with the 0-π boundary at $x = 0$ and equal by (absolute value) critical current densities in 0 and π parts is given by $j_c(x)/j_{c0} = \mathrm{sgn}(x)$.

The second approach is more appropriate for the d-wave based JJs where the phase shift of π takes place not inside the junction itself, but inside the d-wave superconductor, so that the whole

Josephson junction can be considered as a 0 JJ. In this case, again assuming equal critical current densities for all facets, one arrives to the following perturbed sine-Gordon equation [1]:

$$\phi_{xx} - \phi_{tt} - \sin(\phi) = \alpha\phi_t - \gamma(x) + \theta_{xx}(x), \tag{2.4}$$

where $\phi(x,t)$ denotes the Josephson phase across the junction. The function $\theta(x)$ describes the positions of the 0-π boundaries and can be written as

$$\theta(x) = \pi \sum_{k=1}^{N} \sigma_k \mathcal{H}(x - x_k), \tag{2.5}$$

where $\sigma_k = \pm 1$ defines the direction of the k-th phase jump. The sum is over all N 0-π boundaries located at $x = x_k$. $\mathcal{H}(x)$ is the Heaviside step function. Note that since the phase is 2π periodic the direction σ_k of jumps is not important. So, to describe a 0-π-0-π-0-π-... LJJ one can take $\theta(x)$ either changing stepwise as 0, π, 0, π, ... or 0, π, 2π, 3π, ...

It is clear from Eq. (2.4) that if $\theta(x)$ has π jumps at $x = x_k$, then the solution $\phi(x,t)$ will also have π jumps at $x = x_k$. Therefore, x_k are often called a *phase discontinuity points* in the literature.

Since $\theta(x)$ is a sum of steps at different x_k, $\theta_x(x)$ is a sum of δ-functions centered at different x_k, and $\theta_{xx}(x)$ is a derivative of delta functions, i.e. a sum of $-\delta(x - x_k)/(x - x_k)$ functions. It may be quite cumbersome to solve an equation with such terms, especially numerically. To simplify the analysis, it is convenient to present the phase ϕ as a sum of two components: the continuous one $\mu(x)$ and the jumps $\theta(x)$ (2.5), *i.e.*,

$$\phi(x,t) = \mu(x,t) + \theta(x). \tag{2.6}$$

Rewriting Eq. (2.4) in terms of $\mu(x,t)$ we get rid of singular terms:

$$\mu_{xx} - \mu_{tt} - \sin(\mu)\underbrace{\cos(\theta)}_{\pm 1} = \alpha\mu_t - \gamma(x). \tag{2.7}$$

It is rather interesting that this is just the usual perturbed sine-Gordon equation (2.1), but the sign of $\sin(\mu)$ changes from facet to facet. This means that every second facet can be considered as having a negative critical current -1 (in normalized units) instead of $+1$.

Finally, what is the "real" phase, ϕ or μ? It depends on the particular JJ type. In d-wave 0-π JJs the ϕ is the real phase. In SFS-like JJs the real phase is μ. Since one can easily transform Eq. (2.4) into Eq. (2.1) and vice versa using Eq. (2.6) we will use both equations, depending on convenience.

For completeness we give here also the expression for the normalized energy, which, in the presence of phase discontinuities, looks as follows

$$E = \int_0^L \left[\underbrace{\frac{\mu_t^2}{2}}_{\text{kin.(cap.)}} + \underbrace{\frac{\mu_x^2}{2}}_{\text{pot.(ind.)}} + \underbrace{\{1 - \cos[\mu + \theta(x)]\}}_{\text{pot.(Josephson)}} \right] dx. \tag{2.8}$$

The energy is given in units of $E_J = j_c w \lambda_J \Phi_0 / 2\pi$.

2.1.1 Artificial phase discontinuities

Author's contributions: [4, 5]

Is it possible to create a 0-π LJJ (LJJ with π discontinuity) using a conventional LJJ? The information about the position of discontinuities in 0-π LJJ is contained in the $\theta_{xx}(x)$ term. If $\theta(x)$ is a set of steps, then $\theta_x(x)$ is a set of δ-functions, and $\theta_{xx}(x)$ is a set of $-\delta(x - x_k)/(x - x_k)$

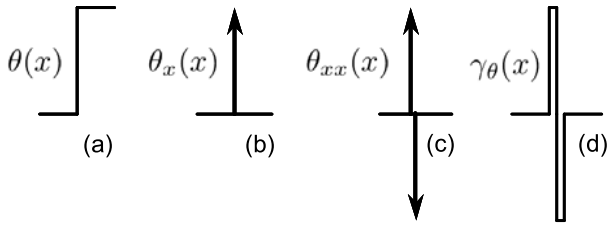

Figure 2.1: $\theta(x)$, $\theta_x(x)$ and $\theta_{xx}(x)$ and its approximation $\gamma_\theta(x)$ by two rectangular pulses of the width Δw and amplitude $\pi/\Delta w^2$ [4].

singularities as shown in Fig. 2.1(a)–(c). If we do not have initially the θ_{xx} term in Eq. (2.4), we can substitute its effect by introducing an additional bias current $\gamma_\theta(x) = \theta_{xx}(x)$. To mimic one π discontinuity the $\gamma_\theta(x)$ profile should be the one shown in Fig. 2.1(c). For practical use, one can approximate it by the profile shown in Fig. 2.1(d). Such a bias profile can be created by two current injectors of width Δw situated at a distance Δx from each other. The current of the amplitude $I_{\rm inj} = \pi I_c \lambda_J/(\Delta w + \Delta x)$ flowing from one injector to another (not through the JJ, but rather only through a tiny part between injectors within the top or bottom superconducting electrode) should create a π discontinuity of the Josephson phase. Thus one can create an artificial 0-π LJJ provided that the width of the whole injector construction $2\Delta w + \Delta x \ll \lambda_J$.

Note that passing different currents, one can create *arbitrary* κ discontinuities ($\kappa \propto I_{\rm inj}$) instead of a π discontinuity, and study arbitrary fractional vortices [2]. This concept was suggested by the author [1] and can be used in the LJJ of any geometry (linear or annular). In a sense, it is a generalization of the idea published a few month earlier [Ust02] to use a pair of current injectors to insert a fluxon (2π-discontinuity) in an annular LJJ. Fractional vortices sitting at a κ discontinuity are discussed in Sec. 2.2.3

In conventional LJJs the phase $\phi = \mu$ is continuous for $I_{\rm inj} = 0$. When we increase $I_{\rm inj}$ the phase ϕ develops a jump $\kappa \propto I_{\rm inj}$ in the vicinity of $x = x_{\rm inj}$. In practice, instead of a jump we have a rapid increase of the phase from some ϕ to $\phi + \kappa$ over a small but finite distance $\Delta x + 2\Delta w$. Physically this means that by passing a rather large current through a piece of the top electrode between two injectors we "twist" the phase ϕ by κ over this small distance, *i.e.*, we insert a squeezed magnetic flux equal to $\kappa\Phi_0/(2\pi)$ into a small distance between injectors. The junction may react on the appearance of such a "discontinuity" by forming a solution $\phi(x)$ [or $\mu(x)$] which changes on the characteristic length λ_J outside the injector area, and corresponds, *e.g.*, to the formation of a fractional Josephson vortex. This technique was suggested already in our first work [1] and then successfully used to investigate various properties of fractional Josephson vortices [4, 11–13].

In the experiment the injectors are never ideal due to technological constraints: they have finite width, and the current flowing from one injector to the other has essentially a 2D distribution. Therefore one has to calibrate the injectors to know the value of injector current needed to create a π discontinuity. The calibration technique for linear LJJ was suggested by us [4]. It is based on measuring the dependence of the critical current I_c of the LJJ on the current through the injectors $I_{\rm inj}$, and comparing the obtained $I_c(I_{\rm inj})$ dependence with the $I_c(\kappa)$ dependence calculated theoretically. It turns out that the $I_c(\kappa)$ dependence in a linear 0-κ LJJ, has minima at $\kappa = \pm\pi$ [4, 5]. Thus, by measuring the value of $I_{\rm inj}$ corresponding to the first minimum of the $I_c(I_{\rm inj})$ dependence we get the calibration coefficient $I_{\rm inj}/\kappa$. Similarly, one can note that the $I_c(\kappa)$ dependence is 2π periodic in κ, therefore one period $\Delta I_{\rm inj}$ of the measured $I_c(I_{\rm inj})$ dependence corresponds to $\kappa = 2\pi$. A typical experimentally measured $I_c(I_{\rm inj})$ dependence is shown in Fig. 2.2. The value of $I_{\rm inj} \approx 13\,{\rm mA}$ corresponds to $\kappa = \pm\pi$.

A similar procedure can be carried out for an annular LJJ. In this case the $I_c(\kappa)$ dependence has a form of Fraunhofer pattern with the first minimum at $\kappa = 2\pi$ [15] [MU04].

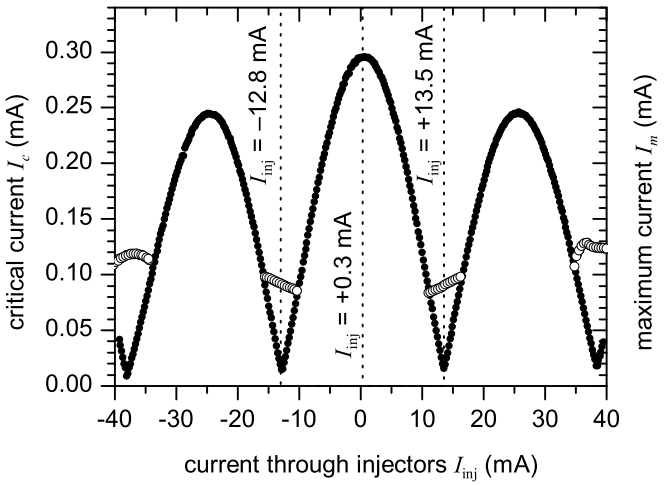

Figure 2.2: Experimentally measured dependence $I_c(I_{\rm inj})$ (solid symbols) and the height $I_{\rm max}(I_{\rm inj})$ of the first half-integer zero field step typical for a *linear* LJJ with finite injector size. Adapted from Ref. [4].

2.2 Ground states

The analysis of the ground states reduces to solving the static version of the sine-Gordon Eq. (2.1) with $\gamma = 0$, *i.e.*,

$$\mu_{xx} = \tilde{j}_c(x)\sin(\mu), \tag{2.9}$$

where $\tilde{j}_c(x) = j_c(x)/j_{c0}$ is the normalized critical current density.

2.2.1 0-π long Josephson junction with a single discontinuity. Semi-fluxon

Author's contributions: [1, 2]

First, consider the simplest situation — an infinitely long JJ with the 0 part for $x < 0$ and the π part for $x > 0$, with equal absolute value of the critical currents in the 0 and π parts, *i.e.*, $|j_c^0| = |j_c^\pi| = j_{c0}$ or $\tilde{j}_c(x) = \mathrm{sgn}(x)$. In this case, the solution of Eq. (2.9), satisfying natural boundary conditions $\mu(-\infty) = 0$ and $\mu(+\infty) = \pm\pi$, is [1]

$$\mu(x) = \pm 4\arctan\left(\mathcal{G}e^{x}\right), \quad x < 0; \tag{2.10a}$$

$$\mu(x) = \pm 4\arctan\frac{1-\mathcal{G}e^{-x}}{1+\mathcal{G}e^{-x}} = \pm\pi \mp 4\arctan\left(\mathcal{G}e^{-x}\right), \quad x > 0, \tag{2.10b}$$

where $\mathcal{G} = \tan(\pi/8) = \sqrt{2} - 1 \approx 0.414$. Since the phase is 2π periodic, $\mu(+\infty) = +\pi$ and $\mu(+\infty) = -\pi$ are equivalent, but lead to two different solutions, if one starts from $\mu(-\infty) = 0$. The solution (2.10) given in terms of the phase $\phi(x)$ can be written in a more compact form as

$$\phi(x) = \mp 4\mathrm{sign}(x)\arctan\left(\mathcal{G}e^{-|x|}\right). \tag{2.11}$$

This solution (with + sign) is shown in Fig. 2.3a. The magnetic field profile is given by $\mu_x(x)$, *i.e.*,

$$\mu_x(x) = \frac{\pm 2}{\cosh(|x| - \ln\mathcal{G})}. \tag{2.12}$$

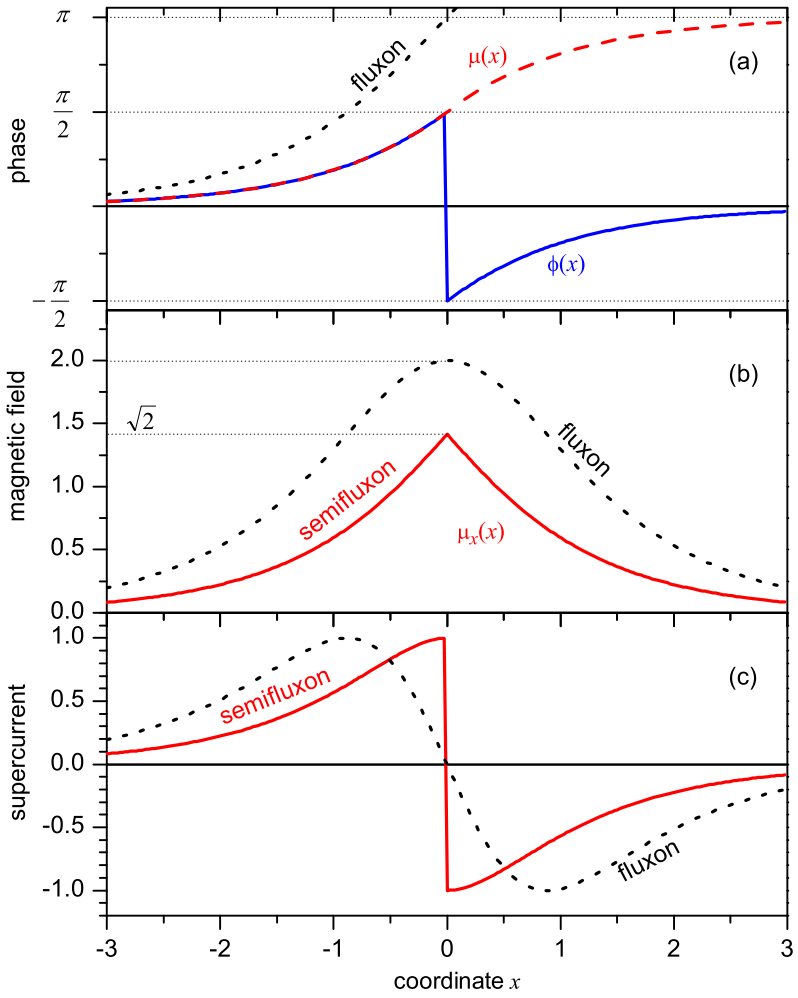

Figure 2.3: Comparison of fluxon and semifluxon shapes. (a) The behavior of the phase $\phi(x)$ and of $\mu(x)$. (b) Magnetic field profile $\mu_x(x)$. (c) Supercurrent profile $\sin(\phi) = \mu_{xx}(x)$.

The field in the center of the semi-fluxon is

$$\mu_x(0) = \frac{\pm 2}{\cosh \ln \mathcal{G}} = \frac{\pm 4}{\mathcal{G} + \frac{1}{\mathcal{G}}} = \pm\sqrt{2}, \tag{2.13}$$

cf., the field $h = \mu_x$ in the center of a fluxon is equal to 2 in normalized units. The normalized magnetic field h is defined as $h = 2H/H_p$, where $H_p = \Phi_0/(\pi\Lambda\lambda_J)$ is the penetration field. The magnetic field profile is shown in Fig. 2.3b. If one calculates the total flux localized at 0-π boundary by integrating the magnetic field over x from $-\infty$ to $+\infty$, one gets π (or $\Phi_0/2$ in physical units), *i.e.*, half of the flux quantum. Therefore, this localized magnetic field is called a *semifluxon*.

The supercurrent density corresponding to a semifluxon can be calculated as

$$\sin(\phi) = \mu_{xx} = \mp 2\,\mathrm{sgn}(x)\frac{\sinh(|x| - \ln \mathcal{G})}{\cosh^2(|x| - \ln \mathcal{G})}, \tag{2.14}$$

and is shown in Fig. 2.3c. One can see that the supercurrent flows through the 0 and π parts of the Josephson barrier in opposite directions. Since we are analyzing the ground state, there is no external bias current applied. Thus the Josephson currents should close somehow. They close by

flowing along the top and bottom electrodes of the LJJ in x direction. As a result a vortex of supercurrent circulating around 0-π boundary is formed. This is a Josephson vortex which has extensions of the order of λ_J in x direction and of the order of λ_L in z direction.

The $\pm$ sign in expressions (2.10)–(2.14) corresponds to two possible solutions: to a semifluxon and to an antisemifluxon. The antisemifluxon has negative sign of the localized magnetic field and supercurrents circulating counterclockwise rather than clockwise.

The energy of a(n) (anti)semifluxon can be calculated by substituting expression (2.10) into Eq. (2.8) to obtain $E_{\rm SF} = 8 - 4\sqrt{2} \approx 2.343$, which is the same for both the semifluxon and the antisemifluxon. Thus, the semifluxon and antisemifluxon form a *degenerate* ground state of the system. For comparison the energy of a fluxon is $E_F = 8$. The energy per unit of LJJ length of a trivial flat phase solution $\mu(x) = 0$ is 0.0 in the 0 part and is 2.0 in the π part. For $\mu(x) = \pi$ it is 2.0 in the 0 part and it is 0.0 in the π part. Thus, having a symmetric 0-π LJJ of the length $L \gg 1$, the energy of any flat phase solution $E_0 = E_\pi = L \gg 1$, which is much larger than the semifluxon energy.

To summarize, a(n) (anti)semifluxon is a Josephson vortex pinned at the 0-π boundary. It forms a degenerate ground state with two possible polarities of the magnetic flux $\pm\Phi_0/2$ corresponding to clockwise or counterclockwise circulation of supercurrent around the 0-π boundary. In this sense, it reminds a classical spin or any other two-state system and we will often use spin notations $\uparrow$ and $\downarrow$ to denote the two different polarities of the semifluxon.

In a real experiment one never has infinite LJJs and the values of critical current densities are not exactly equal, *i.e.*, $j_c^0 \neq j_c^\pi$. The main question which should be answered: what is the ground state of such a LJJ? Will it contain spontaneous magnetic flux in the ground state? The ground state diagram can be calculated and consists of three regions corresponding to the ground state $\mu = 0$, to the state $\mu = \pi$ and to the non-trivial $\mu(x)$ profile. The first two states have flat (constant) phase and, therefore, magnetic field $\mu_x(x) = 0$, i.e. they are fluxless. The third one, is associated with some spontaneous magnetic flux, which depends on the LJJ length L and asymmetry j_c^π/j_c^0 [BKS78, KMS97].

2.2.2 Semifluxon molecules and crystals.

Author's contributions: [2, 3]

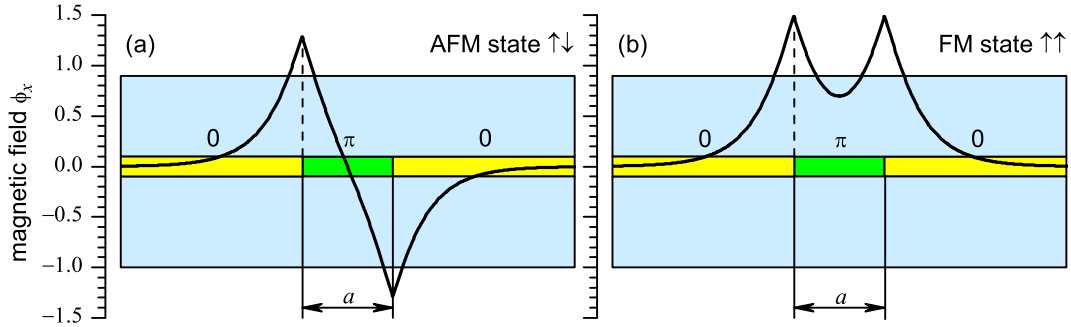

Figure 2.4: Sketch of a 0-π-0 LJJ with (a) AFM ordered semifluxons, state $\uparrow\downarrow$ and (b) FM ordered semifluxons, state $\uparrow\uparrow$.

The next simplest configuration is the 0-π-0 LJJ shown in Fig. 2.4. The LJJ is assumed be of infinite length, while the length of π part in the middle is a, thus $\theta(x) = \pi$ if $|x| < a/2$ and $\theta(x) = 0$ otherwise. The possible static solutions are: $\mu(x) = 0$ ($\phi(x) = \theta(x)$), $\mu(x) = \pi$ ($\phi(x) = \pi + \theta(x)$) and two semifluxons, each sitting at one of the 0-π boundaries, *i.e.*, the states $\downarrow\downarrow$, $\uparrow\uparrow$, $\downarrow\uparrow$, $\uparrow\downarrow$.

Obviously, the energy of the ferromagnetic states $\downarrow\downarrow$ and $\uparrow\uparrow$ is the same. The same is valid for the antiferromagnetic states $\downarrow\uparrow$, $\uparrow\downarrow$. It also can be shown that the energy of the FM states is larger than the energy of the AFM states. Thus, in the ground state, the flat phase state $\mu = 0$ with $E = 2a$ competes with the AFM semifluxon states. It turns out [2, 3] [KI97] that for $a < \pi/2$ the flat phase state $\mu = 0$ is the ground state, while for $a > \pi/2$ the ground state is a degenerate AFM state of two semifluxons.

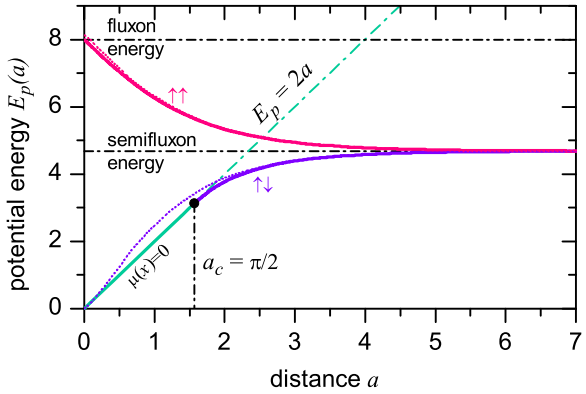

Figure 2.5: The potential energy of various static states as a function of the distance a between 0-π boundaries (length of the π region). The crossover point between the AFM state $\uparrow\downarrow$, and the flat phase state $\mu = 0$ is at $a = a_c = \pi/2$. The energies of FM and AFM states were calculated by solving the sine-Gordon Eq. (2.1) numerically to obtain a static solution $\mu(x)$ and then substituting it into Eq. (2.8). Dotted lines show energies calculated using a simple linear superposition of two semifluxons, Eq. (2.10) with arguments $x \pm a/2$ instead of x, substituted into Eq. (2.8).

The energies of various static solutions as a function of a are shown in Fig. 2.5. Clearly, at $a \to \infty$ the energies of both FM and AFM states are just equal to $2E_{\rm SF}$ as semifluxons do not interact. At small a the shape and the energy of FM state approaches the shape and the energy of an integer fluxon $E_F = 8$. The energy of AFM state decreases as a decreases because semifluxons partially cancel each other. Note that the AFM line ends at $a = \pi/2$, which actually means that the AFM solution smoothly collapses into the $\mu = 0$ state, *i.e.*, *ceases to exist* at $a = \pi/2$. At $a < \pi/2$ the ground state is a flat phase state $\mu(x) = 0$, which has an energy $E_p = 2a$. The flat phase state is continuously connected with AFM state at $a = \pi/2$.

The analysis of ground states was extended to the case of a LJJ with many 0-π regions numerically [2] and analytically [3]. In these works a LJJ of finite length with many facets of the same length a and edge facets of different length b was considered. The critical current density was assumed to be the same (by absolute value) along the whole JJ. It was found that the LJJ with the odd number of 0-π boundaries always has a ground state with some fractional flux. If the LJJ has an even number of 0-π boundaries, there is a crossover distance a_c such that for $a < a_c$ the ground state is fluxless, while for $a > a_c$ the ground state corresponds to an AFM ordered array of fractional magnetic flux localized at the 0-π boundaries. The values of $a_c^{(N)}(b)$ as a function of facet number and the edge facet size was calculated and is shown in Fig. 4 of Ref. [3]. The general tendency in the behavior of a_c is the following. First, the critical facet size a_c decreases with N. Second, the $a_c(b)$ dependence is non monotonous, having a sharp zero at $b = a/2$. Thus, if the edge facets are twice smaller than the inner facets, the ground state of such a 0-π LJJ will always contain a fractional flux.

2.2.3 0-κ long Josephson junction with one discontinuity

Author's contributions: [15]

The ground state analysis described above was generalized to the case of 0-κ, 0-κ-0 and 0-κ-2κ LJJs with arbitrary values of κ between 0 and 2π [15, 16]. In this case, any static solution is a solution of the following equation

$$\mu_{xx} = \sin[\mu + \theta(x)], \tag{2.15}$$

where $\theta(x)$ jumps between 0, κ, 2κ, etc.

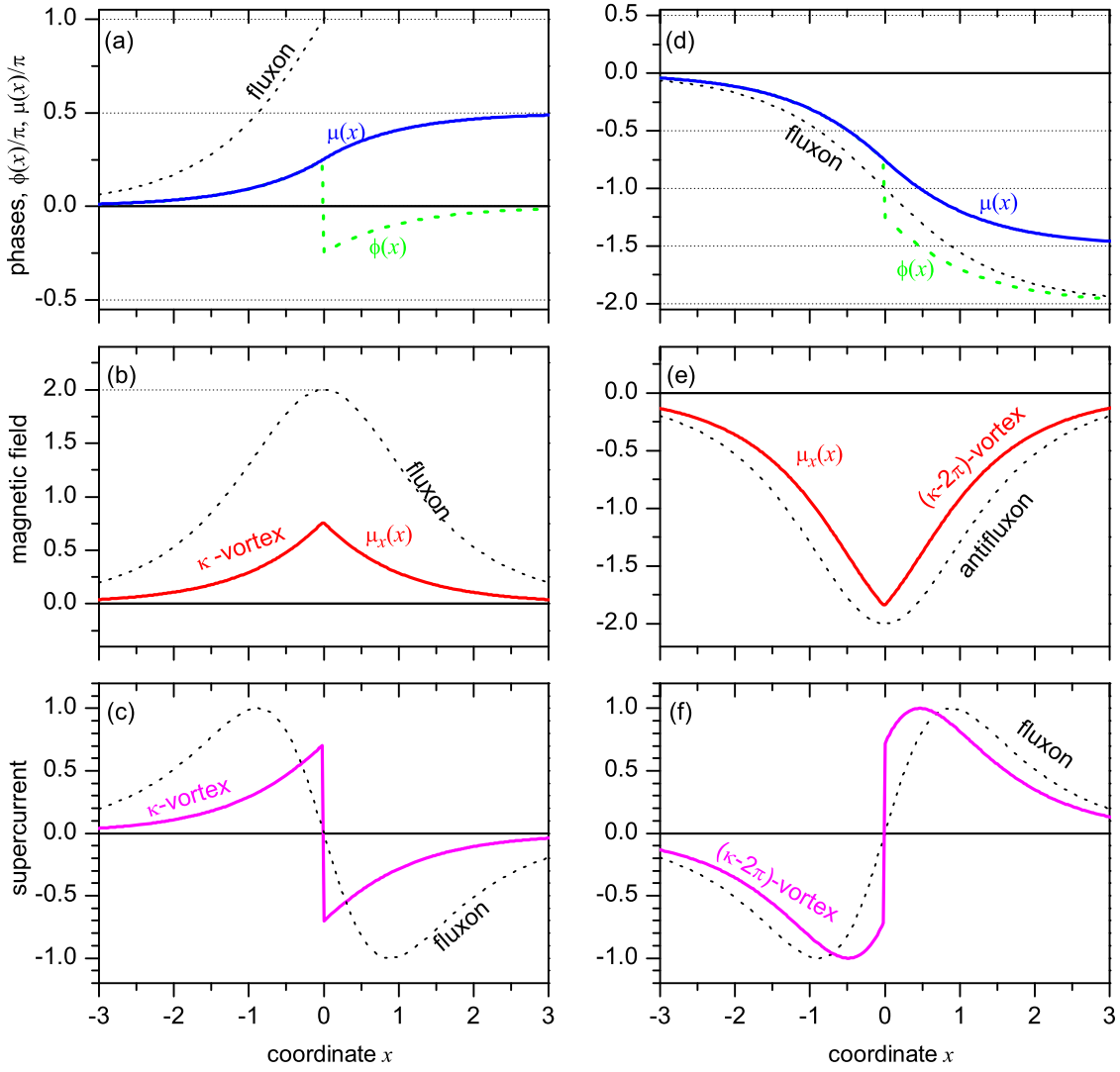

Figure 2.6: Two types of fractional vortices pinned at a $\kappa = \pi/2$ discontinuity. (a)–(c) show the phase, the magnetic field and supercurrents of a direct vortex with topological charge $\wp = -\kappa$. (d)–(f) show the corresponding dependences for complementary vortex with $\wp = 2\pi - \kappa$.

In the case of infinite LJJ, one κ discontinuity of the phase $\phi(x)$ at $x = 0$, results in a phase bending in the λ_J vicinity of $x = 0$, so that at $x \to \pm\infty$ the phase $\phi(x) \to 0$, as shown in Fig. 2.6a. The phase $\mu(x)$ bends smoothly from $\mu(-\infty) = 0$ to $\mu(+\infty) = -\kappa$. Bending of the phase results in the appearance of the localized magnetic field $\mu_x(x)$ and supercurrents $\sin\phi(x) = \sin[\mu(x) + \theta(x)]$, circulating around the κ discontinuity, see Fig. 2.6b,c. The topological charge $\wp$ of such a vortex is equal to $-\kappa$. Thus, the total magnetic flux carried by it is $\Phi = \Phi_0\wp/2\pi = -\Phi_0\kappa/2\pi$.

In fact, the possibility described above is not the only one. Because of the 2π periodicity of the

Josephson phase, one may have solutions $\phi(x)$ that have $\phi(+\infty) = 2\pi k$, where k is an integer. It turns out that one can construct only four such solutions of Eq. (2.15) with $k = 2, 1, 0, -1$, if $0 < \kappa < 2\pi$. It turns out that two of them with $k = 2, -1$ have the topological charge larger than 2π and are unstable. The other two are a *direct* vortex, described above, and a *complementary vortex* with topological charge $-\kappa+2\pi$. A complementary vortex is shown in Fig. 2.6d–f. One can see that, in comparison with a direct vortex, it carries magnetic flux of the opposite sign and has a supercurrent circulating in the opposite direction. Also, direct and complementary vortices are not mirror symmetric as semifluxon and antisemifluxon. Only in the case $\kappa = \pi$ a direct vortex turns into antisemifluxon and the complementary one into a semifluxon.

Note that for $|\kappa| < \pi$ the direct vortex is "lighter", i.e., it carries less flux and has lower energy than a complementary one, which is "heavier". For $\pi < |\kappa| < 2\pi$ it is vice versa. In any case both vortices are stable for any $|\kappa| < 2\pi$. In principle, as a result of some perturbation or manipulation, a heavy vortex may emit a(n) (anti)fluxon and turn into a light vortex provided the fluxon can leave the vicinity of vortex, e.g. through the edges of LJJ or being reabsorbed or pinned by other fractional vortices.

The energy of a direct κ vortex is given by a very simple expression [15]

$$U(\kappa) = 16 \sin^2 \frac{\kappa}{8}. \tag{2.16}$$

2.2.4 Fractional vortex molecules

Author's contributions: [15]

The ground states in 0-κ-0 and 0-κ-2κ LJJs of infinite length were analyzed in Ref. [15]. Note, that if $\kappa \neq \pi$, these two configurations are not equivalent. Further, if the distance a between two discontinuities is large enough (larger than all crossover distances, roughly about $2\lambda_J$, see below), then one may have either direct or complementary vortex sitting at each discontinuity. Thus, one ends up with the following possible ground state configurations.

For $(+\kappa, -\kappa)$ discontinuities with $0 < \kappa < 2\pi$, i.e., a 0-κ-0 LJJ, we may have the following possibilities.

- *Symmetric AFM state*, i.e., two direct vortices $(-\kappa, +\kappa)$ or two complementary ones $(-\kappa + 2\pi, +\kappa - 2\pi)$, denoted as states $\downarrow\uparrow$ and $\uparrow\downarrow$, see Fig. 2d in Ref. [15]. These two states are not stable in the whole range of $0 < \kappa < 2\pi$. Close to $\kappa = \pi$ both states coexist, but closer to $\kappa = 0$ or $\kappa = \pi$ only one of them is stable. Moreover, if $a < \pi/2\lambda_J$, there is a smooth transition between these two states via the flat phase state, see Fig. 3 in Ref. [15].

- *Asymmetric FM state*, i.e., one direct and one complementary vortex in $(-\kappa, +\kappa - 2\pi)$ or $(-\kappa+2\pi, +\kappa)$ degenerate configurations. These states are denoted as $\downarrow\downarrow$ and $\uparrow\uparrow$, respectively, see Fig. 2c in Ref. [15]. Both of them are stable in the whole range $0 < \kappa < 2\pi$.

For $(+\kappa, +\kappa)$ discontinuities with $0 < \kappa < 2\pi$), i.e.. 0-κ-2κ LJJ, we may have the following possibilities.

- *Symmetric FM state* with direct $(-\kappa, -\kappa)$ or complementary $(-\kappa + 2\pi, -\kappa + 2\pi)$ vortices also denoted as $\downarrow\downarrow$ or $\uparrow\uparrow$, see Fig. 2b in Ref. [15]. Symmetric FM states are not stable in the whole range of κ: $(-\kappa, -\kappa) = \downarrow\downarrow$ is stable for $0 < \kappa < \kappa_c^{\downarrow\downarrow}(a) = \kappa_c^{\uparrow\uparrow}(a)$, see Fig. 5a in Ref. [15], while $(-\kappa + 2\pi, -\kappa + 2\pi) = \downarrow\downarrow$ is stable for $2\pi - \kappa_c^{\downarrow\downarrow}(a) = 2\pi - \kappa_c^{\uparrow\uparrow}(a) < \kappa < 2\pi$.

- *Asymmetric AFM state* with one direct and one complementary vortex forming 2-fold degenerate ground state, i.e., $(-\kappa, -\kappa+2\pi)$ and $(-\kappa+2\pi, -\kappa)$ denoted as $\downarrow\uparrow$ and $\uparrow\downarrow$, see Fig. 2a in Ref. [15]. Both states are stable for the whole range of $0 < \kappa < 2\pi$. If the distance a between discontinuities is smaller than some $a_c^{\downarrow\uparrow} = a_c^{\uparrow\downarrow}$, the phase and magnetic field profiles become symmetric with respect to the middle point of the κ part, as shown in Fig. 4 of

Ref. [15]. As $a_c^{\downarrow\uparrow} = a_c^{\uparrow\downarrow}$ are weak functions of κ, one can make transitions to/from such a *symmetric* or *collective* state, by changing $\kappa \propto I_{\rm inj}$ electronically during experiment.

Energies of different fractional vortex molecules as a function of κ are shown in Fig. 6 of Ref. [15]. Transitions between different static configurations upon varying κ are summarized in Fig. 7 of Ref. [15].

2.3 Preparation and readout of vortex states

In order to use semifluxons or fractional Josephson vortices one should be able to perform at least trivial manipulations with them, e.g. set required polarity, using external currents or magnetic fields. One should also be able to read out an unknown state or polarity of a semifluxon. Below we discuss several techniques to do this, mainly focusing on semifluxons. The generalization to the case of arbitrary fractional vortices may easily be done if necessary.

2.3.1 Manipulation of states by the bias current

Author's contributions: [2, 13]

Consider a (formally infinite) 0-π LJJ with the semifluxon in the ground state. If we apply a small positive bias current γ, it exerts a Lorenz force acting on a semifluxon trying to push it to the left. Since the vortex is pinned at the phase discontinuity, it can only deform a little, but not move. If the bias current exceeds the critical value of $\gamma = 2/\pi$, the Lorenz force becomes so strong that it tears off a single fluxon (2π vortex), which accelerates and leaves the vicinity of a discontinuity point. Due to flux conservation, we now have a antisemifluxon localized at the discontinuity point. The bias current acts on it, but exerts the Lorenz force in the opposite direction (to the right). Since the bias is still overcritical, it tears off a whole single antifluxon (-2π vortex), which also moves away, leaving us with a single semifluxon like in the beginning. Obviously this cycle repeats again and again, flipping the semifluxon between up and down states and emitting fluxons to the left and antifluxons to the right. In this way the junction switches to the voltage state. This mechanism was observed numerically by several authors, but was described in details in Ref. [2]. Thus, the critical current of a 0-π LJJ is not equal to $I_{c0} = j_c w L$, but only $I_{c0} \cdot 2/\pi \approx 0.635 I_{c0}$. See Sec. 2.3.2 for more details.

In a 0-π-0 LJJ with the length of the π part $a > a_c = \pi/2$, the AFM molecule $\uparrow\downarrow$ or $\downarrow\uparrow$ is formed in the ground state. If one applies a dc bias current γ such that Lorenz force pushes semifluxons towards each other, at some bias current $\gamma_{\rm RE}$ the two vortices simultaneously flip and change the polarity, i.e. [2],

$$\uparrow\downarrow \overset{\gamma=\gamma_{\rm RE}}{\longrightarrow} \downarrow\uparrow \,. \tag{2.17}$$

The value of $\gamma_{\rm RE} \approx 0.08$ for $a = 2$ and $L = \infty$. The flipping process, during which one flux quantum is transferred from one semifluxon to the other, takes only few plasma periods. The semifluxons in the new AFM molecule have such polarities that the molecule is stretched by the Lorenz force. If one increases the bias current further above $\gamma_c(a)$, the Lorenz force gets so strong that it tears off one fluxon and one antifluxon from the right and from the left ends of a molecule and the junction switches to the non-zero voltage state, similar to the case of a single semifluxon. If, on the other hand, one will not exceed $\gamma_c(a)$, but will decrease the bias down to $-\gamma_{\rm RE}$, the reverse rearrangement will take place

$$\downarrow\uparrow \overset{\gamma=-\gamma_{\rm RE}}{\longrightarrow} \uparrow\downarrow \,. \tag{2.18}$$

Thus, still being in the zero voltage state one can switch the molecule between the states $\uparrow\downarrow$ and $\downarrow\uparrow$ by applying a small positive or negative bias current $|\gamma_{\rm RE}(a)| < |\gamma_c(a)|$. Obviously both $\gamma_{\rm RE}(a)$ and $\gamma_c(a)$ depend on a. For large a, say above $5\lambda_J$, the semifluxons in a molecule almost do not

see each other, so $\gamma_c \to 2\pi$ and $\gamma_{\rm RE} \to \gamma_c$, i.e., it will be impossible to rearrange in practice. In the other extreme case, $a < \pi/2\lambda_J$, the ground state is a flat phase state so, formally, $\gamma_{\rm RE} = 0$ — the domain of bi-stability vanishes. Thus, the optimum distance a for manipulations with an AFM molecule of two semifluxons is about $2 \dots 4\lambda_J$. Such a rearrangement $\uparrow\downarrow \leftrightarrow \downarrow\uparrow$ was recently demonstrated experimentally in a 0-π-0 LJJ of $L = 7.2\lambda_J$ with $a = 2.4\lambda_J$ [13].

In Ref. [2] it was also shown that similar rearrangements can be organized in a longer chain of semifluxons. In this case, the rearrangement takes place in several steps from a perfect AFM state to the completely polarized state. For example, for 12 semifluxons

$$\begin{aligned}
&\uparrow\downarrow\uparrow\downarrow\uparrow\downarrow\uparrow\downarrow\uparrow\downarrow\uparrow\downarrow \overset{\gamma=+0.14}{\longrightarrow} \downarrow\downarrow\downarrow\downarrow\uparrow\downarrow\uparrow\uparrow\uparrow\uparrow\uparrow\uparrow \overset{\gamma=+0.31}{\longrightarrow} \\
&\downarrow\downarrow\downarrow\downarrow\downarrow\uparrow\uparrow\uparrow\uparrow\uparrow\uparrow\uparrow \overset{\gamma=+0.12}{\longrightarrow} \downarrow\downarrow\downarrow\downarrow\uparrow\downarrow\uparrow\uparrow\uparrow\uparrow\uparrow\uparrow \overset{\gamma=+0.00}{\longrightarrow} \\
&\downarrow\downarrow\uparrow\downarrow\uparrow\downarrow\uparrow\uparrow\downarrow\uparrow\uparrow \overset{\gamma=-0.05}{\longrightarrow} \uparrow\uparrow\downarrow\uparrow\downarrow\uparrow\downarrow\uparrow\downarrow\downarrow \overset{\gamma=-0.18}{\longrightarrow} \\
&\uparrow\uparrow\uparrow\uparrow\uparrow\downarrow\uparrow\downarrow\downarrow\downarrow\downarrow\downarrow \overset{\gamma=-0.31}{\longrightarrow} \uparrow\uparrow\uparrow\uparrow\uparrow\uparrow\downarrow\downarrow\downarrow\downarrow\downarrow\downarrow
\end{aligned} \tag{2.19}$$

with $\gamma_c = +0.47$ from the state $\downarrow\downarrow\downarrow\downarrow\downarrow\uparrow\uparrow\uparrow\uparrow\uparrow\uparrow$. We also checked that the situation is symmetric, *i.e.*, $\gamma_c = -0.47$ from the state $\uparrow\uparrow\uparrow\uparrow\uparrow\uparrow\downarrow\downarrow\downarrow\downarrow\downarrow\downarrow$. If we start from the state $\downarrow\downarrow\uparrow\downarrow\downarrow\uparrow\downarrow\uparrow\uparrow\downarrow\uparrow\uparrow$ at $\gamma = 0$ obtained in (2.19), and increase γ, we get some new states which we have not seen before [2]:

$$\downarrow\downarrow\uparrow\downarrow\downarrow\uparrow\downarrow\uparrow\uparrow\downarrow\uparrow\uparrow \overset{\gamma=+0.12}{\longrightarrow} \downarrow\downarrow\downarrow\uparrow\downarrow\uparrow\downarrow\uparrow\downarrow\uparrow\uparrow\uparrow\uparrow \overset{\gamma=+0.19}{\longrightarrow} \downarrow\downarrow\downarrow\downarrow\downarrow\uparrow\uparrow\uparrow\uparrow\uparrow\uparrow$$

Interesting enough, similar rearrangements are possible even when the initial state at $\gamma = 0$ is flat. For example, for 6 semifluxons separated by the distance $a = 1$ we get

$$\text{------} \overset{\gamma>+0.00}{\longrightarrow} \downarrow\uparrow\downarrow\uparrow\downarrow\uparrow \overset{\gamma=+0.37}{\longrightarrow} \downarrow\downarrow\ \text{--}\ \uparrow\uparrow \tag{2.20}$$

with $\gamma_c = 0.48$ from the state $\downarrow\downarrow$--$\uparrow\uparrow$.

Experimentally, manipulation the flipping between $\uparrow\downarrow$ and $\downarrow\uparrow$ controlled by bias current was reported by us [13] and is presented in detail in Sec. 2.3.3

2.3.2 $I_c(H)$ and $I_c(I_{\rm inj})$ as a tool to study semifluxon states

$I_c(H)$ dependence in 0-π LJJ

In a conventional LJJ the behavior of maximum supercurrent as a function of magnetic field, further denoted as $I_c(H)$, is a good characterization tool, which gives information about the uniformity of the LJJ and about the presence of a background magnetic field or parasitic trapped magnetic flux. The $I_c(H)$ in 0-π LJJ can give even more information, in particular about semifluxon states, and is invaluable tool for characterization of 0-π LJJ and determination of its internal flux states. The $I_c(H)$ dependence in a 0-π LJJ was studied in several works. In the following it is assumed that the magnetic field is applied in the plane of the junction along its y direction, i.e., perpendicular the junction length L (x direction).

For the short 0-π LJJ it was shown [VH95, KMS97] that

$$I_c(H) = I_{c0} \left| \frac{\sin^2(\pi\Phi/2\Phi_0)}{\pi\Phi/2\Phi_0} \right|, \tag{2.21}$$

where $I_{c0} = j_c L w$ is the *intrinsic* critical current of the junction, L is the junction length and w is width, while $\Phi = HL\Lambda$ is the flux threading the effective LJJ area, Λ being the effective magnetic thickness of the LJJ. In comparison with the Fraunhofer dependence, the dependence (2.21) has a cusp-like minimum at $H = 0$ ($\Phi = 0$). The formula (2.21) was generalized to the case of a 0-π-0-π-... LJJ with many facets, but still in the short limit [SAB+02]. Comparison with experiments on $YBa_2Cu_3O_7$-Nb and $Nd_{2-y}Ce_yCuO_x$-Nb ramp zigzag junctions having between 8 and 40 facets shows good qualitative agreement between experiment and derived formula. [SAB+02, ADS+05]

For an infinitely long ($L = \infty$) 0-π LJJ, the shape of $I_c(H)$ dependence was predicted by several authors [XMT95, KMS97, Laz04]. Since uniform magnetic field penetrates from the edges (i.e. far from 0-π boundary with a semifluxon), it is predicted to be similar to the usual $I_c(H)$ pattern of a 0 LJJ at least for the case when no fluxons have penetrated inside the LJJ yet [XMT95]. A $I_c(H)$ dependence for 0 LJJ at small fields has a triangular shape

$$I_c^0(H, \infty) = I_{c0}\left(1 - \frac{H}{H_{c1}}\right), \quad H < H_{c1}, \tag{2.22}$$

where H_{c1} is a penetration field. It turns out that one should also take into account that if the uniform bias current exceeds the depinning current of a semifluxon $(2/\pi)I_{c0}$, then the junction switches to the resistive state [2, 3] — the argument which was missed in Ref. [XMT95]. Thus, $I_c(H)$ looks like a pattern (2.22) cut off from the top at $(2/\pi)I_{c0}$:

$$I_c^{0\text{-}\pi}(H, \infty) = I_{c0} \max\left[\left(1 - \frac{H}{H_{c1}}\right), \frac{2}{\pi}\right], \quad H < H_{c1}. \tag{2.23}$$

For intermediate LJJ length one observes a smooth transition from the curve (2.21) to (2.23), qualitatively similar for inline [KMS97] and overlap [Laz04] geometry.

Recently, a detailed analysis of stability boundaries of different solutions was performed [AB07]. This analysis provided several important statements.

- One can observe a hysteresis between different branches of the $I_c(H)$ dependence, e.g., a semifluxon branch and antisemifluxon branch. The experimental observation of a hysteresis at least around the intersection point of these branches, is an evidence of a bi-stable solution, i.e. existence of semifluxons of two polarities.
- In addition to symmetric states such as ↑, ⇑↑⇑, ⇑⇑↑⇑⇑, etc., one can have asymmetric states, such as ⇑↑, ⇑⇑↑, ⇑⇑↑⇑, etc even in an absolutely symmetric LJJ. Such asymmetric fluxon states manifest themselves as rather flat branches on the $I_c(H)$ dependence that appear between side maxima of $I_c(H)$. In an asymmetric 0-π LJJ such flat branches are more pronounced on one of the sides (in H) of the $I_c(H)$ dependence.
- the $I_c(H)$ dependence can give information about asymmetries of 0-π LJJ. For example, in a perfectly symmetric 0-π LJJ of a given length l, the central minimum is located at $H = 0$, and has a critical current $I_c(0, l)$ which is a known, numerically calculated function of l. The first side maxima have the amplitude $\approx 0.72 I_{c0}$ [VH95, KMS97, SAB+02]. If one considers an asymmetric LJJ, e.g., with $j_c^\pi / j_c^0 \neq 1$ as a measure of asymmetry, one will find out that the central minimum is situated at $H \neq 0$, has different I_c, and the first side maxima amplitudes are not equal. By determining these parameters from experimental $I_c(H)$ curves one may be able to recover the parameters of the 0-π LJJ and, in particular, determine the asymmetry between 0 and π parts.

$I_c(I_{\text{inj}})$ dependence

Author's contributions: [4–6]

The dependence of the critical current on the value of discontinuity κ (in experiment on the injector current amplitude I_{inj}) plays an important role for injector calibration, for manipulation of the fluxon states, for understanding critical currents and pinning in 0-κ LJJs.

For a linear 0-π LJJ with one discontinuity in the center the $I_c(I_{\text{inj}})$ dependence was for the first time derived to perform an injector calibration [4, 5]. For $l \ll 1$ and $l \gg 1$ the $I_c(I_{\text{inj}})$ dependence can be presented in analytical form. For $l \sim 1$ one should calculate $\gamma_c(\kappa)$ numerically. The dependence is 2π periodic in κ and exhibits *a cusp-like minimum at* $\kappa = \pi$. The branch with $\kappa \in [-\pi, \pi]$ corresponds to a direct $-\kappa$ vortex sitting at the $+\kappa$ discontinuity. For $\kappa > 0$

this vortex has a negative flux $-\Phi_0\kappa/2\pi$ (vorticity $-\kappa$), while for $\kappa < 0$ this flux is positive. The branch with $\kappa \in [\pi, 3\pi]$ corresponds to a complementary $\kappa - 2\pi$ vortex sitting at the $+\kappa$ discontinuity. For $\kappa < 2\pi$ its flux is negative, for $\kappa > 2\pi$ it is positive. For $\kappa = 2\pi$ the flux is zero — a 2π discontinuity is equivalent to no discontinuity (in a linear LJJ, where extra fluxons can be created and emitted).

If one measures a $I_c(I_{\rm inj})$ dependence in experiment, the position of the first cusp-like minimum will determine the value of $I_{\rm inj}$ needed to create $\kappa = \pi$ discontinuity. Note, that in experiment, due to the finite size of the injectors, the $I_c(I_{\rm inj})$ dependence deviates a bit from the shape predicted theoretically, e.g. the critical current in the maxima number $n = \pm 1$ is lower than for $n = 0$. Such deviations are rather well understood [5].

For a linear LJJ with two $(+\kappa, -\kappa)$ discontinuities placed at a distance a from each other symmetrically with respect to the junction length the $I_c(\kappa)$ dependence was used to calibrate injectors in a semifluxon molecule rearrangement experiment [13]. Here the $I_c(\kappa)$ dependence is also 2π periodic, but skewed so that the cusp-like minimum, in general, does not correspond to $\kappa = \pm\pi$. In this case, one can find $I^{\pi}_{\rm inj}$by measuring both positive $I_{c+}(I_{\rm inj})$ and negative $I_{c-}(I_{\rm inj})$ critical currents and plotting their absolute values $|I_{c\pm}(I_{\rm inj})|$ on the same plot. Then, the intersection points in the vicinity of the first minima will give the value of $I^{\pi}_{\rm inj}$.

For annular 0-π LJJ with one discontinuity point, the $I_c(\kappa)$ dependence turns out to be the well known Fraunhofer pattern with the first minimum at $\kappa = 2\pi$ [6] [MU04]. Imagine that at $\kappa = 0$ the phase $\phi(x) = 0$. As κ grows from 0, a fractional $-\kappa$ vortex is induced to compensate a $+\kappa$ discontinuity. At $\kappa = 2\pi$ this vortex is an antifluxon which can detach from a discontinuity and move to some other location inside the ALJJ. If one applies an infinitesimally small bias current, it exerts a Lorenz force on an antifluxon, the antifluxon starts moving, producing nonzero average voltage across the ALJJ. Thus the critical current is zero. This technique was initially suggested to controllably insert an integer fluxon into an ALJJ [Ust02, MU04], but obviously can be used to create an arbitrary phase discontinuity κ and study direct and complementary vortices sitting at it, just like in the linear LJJ above. The only difference between the linear and annular cases is that in the annular case the total topological charge is conserved, so that $\kappa = 3\pi$ is not equivalent to $\kappa = \pi$, but equivalent to $\kappa = \pi$ *plus* a 2π fluxon situated somewhere in the junction.

It turns out that pinning of fluxons by fractional vortices completely follows from the Fraunhofer $I_c(\kappa)$ dependence [6]. In fact, the central lobe of this dependence with $-2\pi < \kappa < +2\pi$ gives a depinning current of a fractional vortex with the topological charge $-\kappa$. The first order side lobes with $2\pi < |\kappa| < 4\pi$ correspond to the (de)pinning of a fluxon or antifluxon pinned by a fractional vortex of the same polarity with the topological charge $\pm(|\kappa| - 2\pi)$. The second order side lobes with $4\pi < |\kappa| < 6\pi$ correspond to the (de)pinning of two fluxons or two antifluxons by a fractional vortex with the topological charge $\pm(|\kappa| - 4\pi)$, and so on [6].

2.3.3 SQUID readout (non-destructive)

Author's contributions: [13]

The most direct way to monitor the semifluxon (molecule) states is to measure magnetic flux localized in the vicinity of a phase discontinuity or 0-π boundary, e.g., using a dc SQUID. The flux sensitivity of a typical SQUID can easily be $\sim 10^{-3}\Phi_0$, so that it is enough to detect fluxes $\sim \Phi_0/2$ even if the flux coupling is of the order of $1 \ldots 10\%$. In a series of pioneering works, the dc SQUID was put on the tip of a SQUID microscope and was moved above the surface of the sample to measure local magnetic fields. In this way the first images of semifluxons were obtained [KTM99, HAS+03, KTA+05]. In these works, the magnetic field of the semifluxons was directed perpendicular to the surface of the sample and was detected by the SQUID loop situated in the plane of the sample. In the case of SFS/SIFS 0-π LJJs or SIS LJJs with artificial phase discontinuities, the magnetic field of a semifluxon is directed in-plane (and then closes out of plane) so that interpretation of images will require some efforts. The disadvantage of this technique is that one needs a rather unique low temperature scanning SQUID microscope which exists only in

few labs in the world.

Another possibility is to fabricate the SQUIDs directly on-chip together with the 0-π LJJ: one SQUID next to each 0-π boundary. The geometry should provide reasonable coupling of the order of $1 \ldots 10\%$ between the flux of a semifluxon and the SQUID loop. Usually this is achieved using a specially designed pick up loop. The advantages of on-chip SQUIDs are the following. First, the SQUIDs can be fabricated using the same JJ process as for 0-π LJJs. Second, one can design coupling loops for any direction of semifluxon field. The disadvantage is that one can detect only the total flux contained in a semifluxon, but not its spatial profile. Thus, on-chip SQUIDs are more useful in digital electronic devices to detect switching between different semifluxon states, e.g., as described in Sec. 2.3.1.

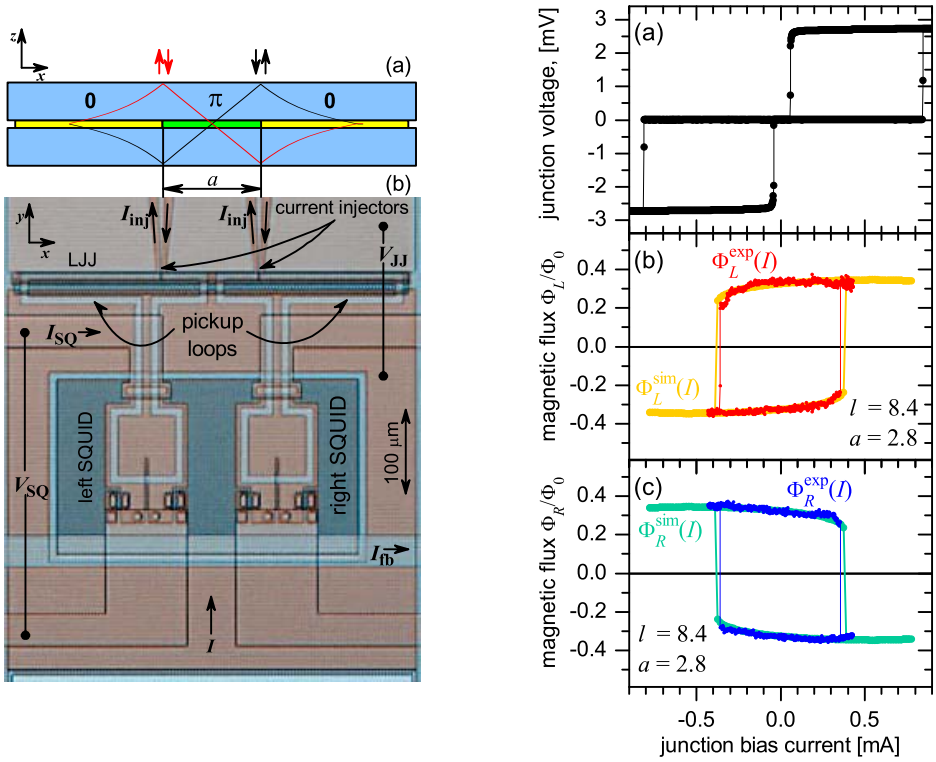

Figure 2.7: (Left) Sketch of the LJJ and an optical picture of the sample used for manipulation and read-out of two-semifluxon molecule states. (Right) $V(I)$ curve (a) and fluxes $\Phi_L^{\rm exp}(I)$ (b) and $\Phi_R^{\rm exp}(I)$ (b) detected by the left and the right SQUIDs, accordingly. Numerically simulated flux dependences $\Phi_L^{\rm sim}(I)$ (b) and $\Phi_R^{\rm sim}(I)$ (b) are shown also. Adapted from Ref. [13]

Recently we have demonstrated an on-chip SQUID readout of two-semifluxon molecule states, which could be controllable manipulated between $\uparrow\downarrow$ and $\downarrow\uparrow$ states by applying under-critical bias current [13]. In Fig. 2.7 one can see the setup used for this experiment as well as main experimental results. On the top of the picture one sees a LJJ equipped with a pair of current injectors to create 0-π-0 LJJ electronically and arrive to one of the states $\uparrow\downarrow$ or $\downarrow\uparrow$. The critical current of the IVC in Fig. 2.7(a) corresponds to a depinning of the molecule. If one sweeps the bias current I back and forth with the amplitude *not* exceeding $I_c(I_{\rm inj})$, one sees no voltage on the IVC, but the state of both readout SQUIDs changes at $I \approx \pm 0.36\,$mA, corresponding to the rearrangement between the states $\uparrow\downarrow$ and $\downarrow\uparrow$. This technique was also used to map the bistability boundary of a molecule consisting of arbitrary fractional vortices [13] and can also be used in quantum domain.

2.3.4 Test fluxon readout (destructive)

Another possibility to read out an unknown state of a single semifluxon is to inject an integer fluxon of known polarity and observe the result of their interaction. As an example, consider a semifluxon of unknown polarity. The polarity can be positive like in Fig. 2.8a or negative like in Fig. 2.8b. To determine it, we inject a single fluxon of positive polarity somewhere to the left from semifluxon. This injection can be done using injectors or using an RSFQ-like circuit (DC-SFQ converter). Then we increase the bias current slowly. The semifluxon stays pinned, but the fluxon moves to the right and interacts with the semifluxon.

If both the fluxon and the semifluxon are of the same polarity, as shown in Fig. 2.8a, they repel each other so that the fluxon sticks being pinned by a semifluxon. Only when the bias current exceeds the depinning current of $(2/3\pi)I_{c0} \approx 0.21I_{c0}$ the fluxon depins and passes through, as indicated in Fig. 2.8a. In an annular LJJ this will be detected as a voltage due to fluxon motion around the annulus. In a linear LJJ one can attach a RSFQ fluxon detection circuit (SFQ-DC converter) to the right hand side of the LJJ.

If the fluxon and the semifluxon have opposite polarities as shown in Fig. 2.8b, they simply annihilate, resulting an semifluxon pinned at the 0-π boundary, see Fig. 2.8b. Further increase of the bias will depin the semifluxon and produce a voltage only when the bias exceeds $(2/\pi)I_{c0} \approx 0.63I_{c0}$.

Thus, by injecting a test fluxon of known polarity at $I = 0$ and measuring the critical current of the LJJ, we get two possible values (corresponding to two semifluxon states), which differ from each other as much as three times. Although this method looks rather simple in case of a single semifluxon, it is quite complicated to use it to readout the states of a semifluxon molecule. In the best case, one can only readout the total number of fluxons or antifluxons in a molecule, but not their mutual position.

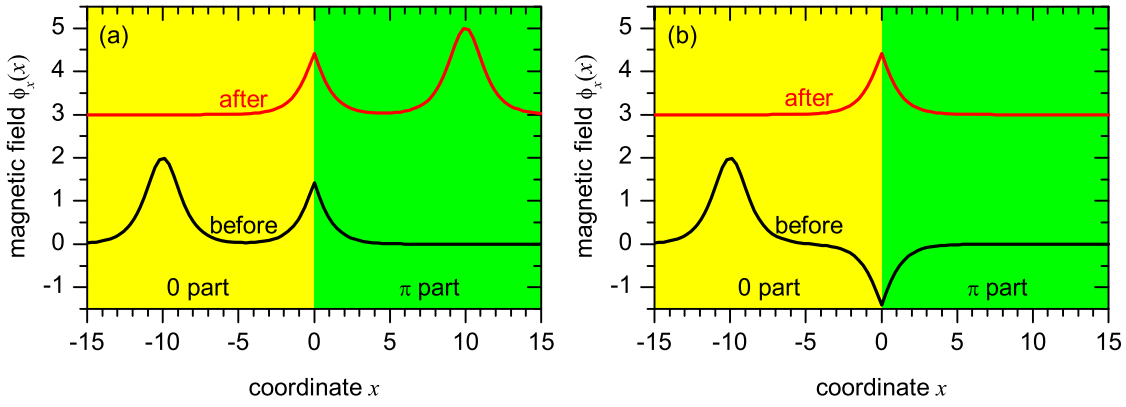

Figure 2.8: Schematic demonstration of readout of unknown semifluxon state using a test fluxon of positive polarity. The interaction of test fluxon with (a) positive and (b) negative semifluxon are shown.

2.4 Eigenmodes of fractional vortices

In Sec. 2.2 we have considered several fractional vortex configurations which are solutions of the static sine-Gordon equation. Actually, the stability of each such solution should be checked separately. Moreover, the stability analysis will allow to find eigenfrequencies of vortex oscillations around equilibrium. The stability analysis is performed following the standard procedure. First, we take any static solution $\mu_s(x)$ (obtained numerically or analytically) which we would like to investigate. Then, we suppose that it is perturbed due to thermal fluctuations or other external

influences so that the phase in the LJJ is given by

$$\mu(x,t) = \mu_s(x) + \varepsilon(x,t) = \mu_s(x) + \varepsilon(x)e^{\lambda t} \tag{2.24}$$

which should be a new solution of sine-Gordon equation. Here we assume that the perturbation $\varepsilon(x,t)$ has some spatial profile $\varepsilon(x)$, while its amplitude increases [$\mathrm{Re}(\lambda) > 0$] or decreases [$\mathrm{Re}(\lambda) < 0$] exponentially and may also oscillate [if $\mathrm{Im}(\lambda) \neq 0$]. Substituting the expression (2.24) into the sine-Gordon Eq. (2.1), we obtain the equation for perturbation

$$\varepsilon_{xx} - j_c(x)\cos[\mu_0(x)]\varepsilon = \Lambda\varepsilon. \tag{2.25}$$

Assuming that α is not a function of x, we have introduced a new eigenvalue variable Λ instead of λ:

$$\Lambda = \lambda^2 + \alpha\lambda. \tag{2.26}$$

If we will be able to find a spectrum Λ_i of Λ in Eq. (2.25), the corresponding λ_i are given by

$$\lambda_i^{\pm} = \frac{-\alpha \pm \sqrt{\alpha^2 + 4\Lambda_i}}{2}. \tag{2.27}$$

Note that a pair of complex conjugate $\lambda_i^{\pm}$ or a pair of real $\lambda_i^{\pm}$ may correspond to one Λ_i. If there is at least one $\Lambda_n > 0$, then $\lambda_n^{+} > 0$ and the system is unstable. On the other hand, if all $\Lambda_i < -\alpha^2/4$, then all $\lambda_i^{\pm}$ are complex conjugate with $\mathrm{Re}(\lambda_i) = -\alpha/2 < 0$ and the system is stable. In the last case, when some of the Λ_i lay in the interval $-\alpha^2/4 < \Lambda_i < 0$ and the others have $\Lambda < -\alpha^2/4$, $\lambda_i^{\pm}$ are two real negative eigenvalues and the system is stable again. Thus, we conclude that the system is stable if all $\Lambda_i < 0$, and *the damping α does not affect stability* of our system. What *damping does affect* is the presence and *the number of the eigenfrequencies* $\omega_{0,i} = |\,\mathrm{Im}(\lambda_i)|$. If some of the Λ_i lay in the interval $-\alpha^2/4 < \Lambda_i < 0$, then the system will have no eigenfrequencies corresponding to these Λ_i in the presence of damping, but if the damping is switched off, eigenfrequencies will appear.

To solve Eq. (2.25) numerically we discretize it along x with the uniform step Δx. Then the eigenvalue problem (2.25) can be written in a matrix form

$$\mathbf{A}\cdot\boldsymbol{\varepsilon} = \Lambda\boldsymbol{\varepsilon}, \tag{2.28}$$

where $\boldsymbol{\varepsilon}$ is an N-dimensional vector with the components $\varepsilon_i = \varepsilon(x_i)$ and $\mathbf{A}$ is an $N \times N$ matrix, where $N = L/dx$ can be rather large. Practically tractable sizes are of the order 4000×4000. To solve the eigenvalue problem (2.28) we can use several standard numerical approaches depending on the content of the matrix (tri-diagonal, symmetric or general). As a result one obtains a vector of eigenvalues Λ, which contains N complex values.

2.4.1 Stability and eigenfrequencies of different vortex states

Author's contributions: [11, 12, 16, 25]

Using the approach outlined above one can investigate the stability of various static solutions of Eq. (2.1). A phase of a single fractional $\wp$ vortex sitting at $x_0 = 0$ in an infinite LJJ is given by [15]

$$\mu_0(x) = \begin{cases} \phi_0(x - x_0), & x < 0, \\ \wp - \phi_0(-x - x_0), & x > 0, \end{cases}, \tag{2.29}$$

where $\phi_0(x)$ is a soliton (fluxon) solution

$$\phi_0(x) = 4\arctan e^x, \tag{2.30}$$

and

$$x_0 = -\ln\tan\frac{\wp}{8} > 0. \tag{2.31}$$

The stability analysis in this case can be done analytically. It turns out that all eigenvalues have $\mathrm{Re}(\lambda) < 0$, *i.e.*, the fractional vortex solution is stable. The imaginary parts $\mathrm{Im}(\lambda_i) = \omega_i$ define a set of eigenfrequencies. This set consists of a single discrete eigenfrequency $0 < \omega_0(\wp) < \omega_p$ and a continuous spectrum of frequencies $\omega > \omega_p$. At $\alpha = 0$ the lowest eigenfrequency is given by [16]

$$\omega_0(\wp) = \sqrt{\frac{1}{2}\cos\frac{\wp}{4}\left(\cos\frac{\wp}{4} + \sqrt{4 - 3\cos^2\frac{\wp}{4}}\right)}. \tag{2.32}$$

This frequency corresponds to a wave vector $k = 0$ of the oscillating wave i.e. to a standing wave. The eigenfunction $\varepsilon(x)$ corresponding to this lowest eigenvalue, according to the Sturm-Liouville theorem, has no zeros. Thus, a fractional Josephson vortex with the topological charge $-2\pi < \wp < 2\pi$ has a *localized eigenmode* with the eigenfrequency ω_0 given by Eq. (2.32), see also Fig. 1 of Ref. [16]. At $\wp \to \pm 2\pi$ the eigenfrequency $\omega_0(\wp) \to 0$, indicating an instability at the point $\wp = 2\pi$ when a fractional vortex turns into fluxon, which detaches from the discontinuity point and may freely travel along the LJJ away from the discontinuity point.

Formally, one can also have *more heavy vortices*, with topological charge $|\wp| > 2\pi$, sitting at κ discontinuity as a solution of the static sine-Gordon equation. For example, if $0 < \kappa < 2\pi$, these are $\wp = \kappa + 2\pi$ (positive) and $\wp = \kappa - 4\pi$ (negative) vortices. In case $\kappa = \pi$ they will correspond to the magnetic flux $\pm\frac{3}{2}\Phi_0$. The magnetic field profile inside such heavy vortices has a minimum at the center and then two side maxima. Stability analysis shows that such heavy vortices are *unstable* [16]. They emit a single (anti-)fluxon and downgrade to a smaller fractional vortex, which is stable. One can also see that this decay process is possible by analyzing the energies of initial and final states using Eq. (2.16). [15]

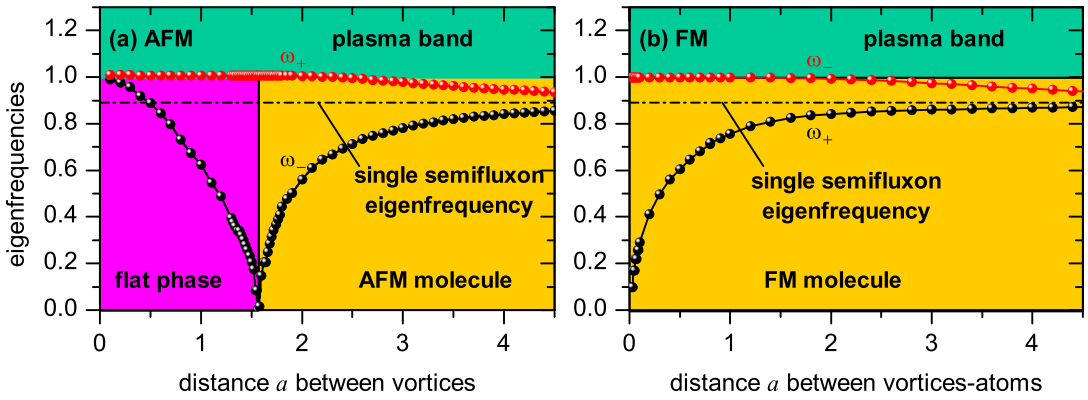

Figure 2.9: Two lowest eigenfrequencies for (a) AFM and (b) FM molecule of two coupled semifluxons as a function of the distance a between them. The 0-π-0 LJJ used for numerical calculations has the length $L = 40\lambda_J$ to emulate an infinite LJJ.

The stability and eigenfrequencies of fractional vortex molecules was also investigated [16]. In this case, analytic approach is rather difficult and one has to use numerics. In the case of two-vortex molecules, the eigenfrequency of individual vortices split as the coupling between the vortices increases (distance a decreases) – just like for two coupled oscillators. As an example, in Fig. 2.9 we present two lowest eigenfrequencies (localized modes) of a AFM- and FM-ordered semifluxon molecules as a function of the distance a between semifluxons.

In the case of AFM molecule, the eigenfrequencies are equal to the ω_0 of a single semifluxon when the distance a is large. If a becomes smaller the eigenfrequency splits into ω_+ and ω_- corresponding to in-phase and out-of-phase oscillations of *magnetic flux* of two vortices. At $a = a_c = (\pi/2)\lambda_J$ the splitting is as large as the plasma gap: $\omega_- \to 0$, indicating an instability of the AFM configuration; the second eigenmode ω_+ joins the plasma band at $a = a_c$. For $a < a_c$, only a flat phase solution $\mu_0 = 0$ exists and is stable. It has only a single eigenfrequency within the gap. Note also that if

one now increases a the flat phase state becomes unstable at the same value of $a = a_c$.

For a FM molecule the situation is similar, but no structural rearrangement occurs at $a = a_c$ as FM state is stable for any a. In this case the in-phase mode frequency $\omega_+ < \omega_-$. At $a \to 0$, where two semifluxons almost form a fluxon, $\omega_+ \to 0$ indicating that a fluxon may depin and move away, *i.e.*, a structural rearrangement takes place.

The eigenfrequencies of various fractional vortex molecules were investigated as a function of κ for different a [16]. The general behavior is quite universal. The eigenfrequencies split as the coupling between vortices increases. Lowest eigenfrequency touches zero at the point of instability of the current state.

The value of eigenfrequency also depends on the value of the bias current γ. Although γ does not explicitly present in Eq. (2.25), it changes $\mu_0(x)$. The dependence of $\omega_0(\gamma)$ is not known analytically, but numerical calculations show that $\omega_0(\gamma)$ decreases as γ increases reaching 0 at the critical or rearrangement current. For a single fractional vortex in infinite 0-π LJJ this dependence can be well approximated by the formula

$$\omega_0(\wp, \gamma) \approx \omega_0(\wp, 0) \sqrt[4]{1 - \left(\frac{\gamma}{\gamma_c(\kappa)}\right)^2}, \tag{2.33}$$

where

$$\gamma_c(\wp) = \frac{I_c(\wp)}{I_{c0}} = \frac{I_c(\wp)}{j_c w L} = \frac{\sin(\wp/2)}{\wp/2}, |\wp| \leq 2\pi \tag{2.34}$$

is the normalized critical current of the junction (depinning current of the fractional vortex) at given κ [NLC02, MU04] [6]. Approximation (2.33) differs from the exact numerical solution by only few percent [except for $\gamma \to \gamma_c(\wp)$], and follows the same functional dependence as the plasma frequency of a small JJ [FD74, DMEC84]

$$\omega_p(\gamma) = \omega_{p0} \sqrt[4]{1 - \gamma^2}, \tag{2.35}$$

i.e., the Eq. (2.33) is exact for $\kappa = 0$. It can serve as a guide for planning and performing the experiment.

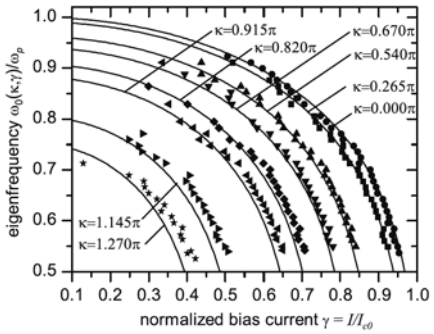

Figure 2.10: Summary of experimentally obtained eigenfrequencies $\omega_0(\gamma)$ for different values of $\wp \propto -\kappa$ (symbols). The lines show the corresponding $\omega_0(\gamma)$ dependences obtained numerically. Adapted from Ref. [11].

Experimentally the eigenfrequency spectroscopy for a single fractional vortex in an annular LJJ with artificial phase discontinuities was performed as a function of discontinuity κ and bias current γ [11, 12]. The result can be seen in Fig. 2.10. The measurements were performed at $T = 4.2K$ by using a resonant escape technique. The annular geometry was chosen to have a possibility to measure vortices with the topological charge $\wp > \pi$. In linear LJJs such vortices can emit a flux and turn into more lighter $\wp - 2\pi$ vortex after the first measurement. As can be seen in

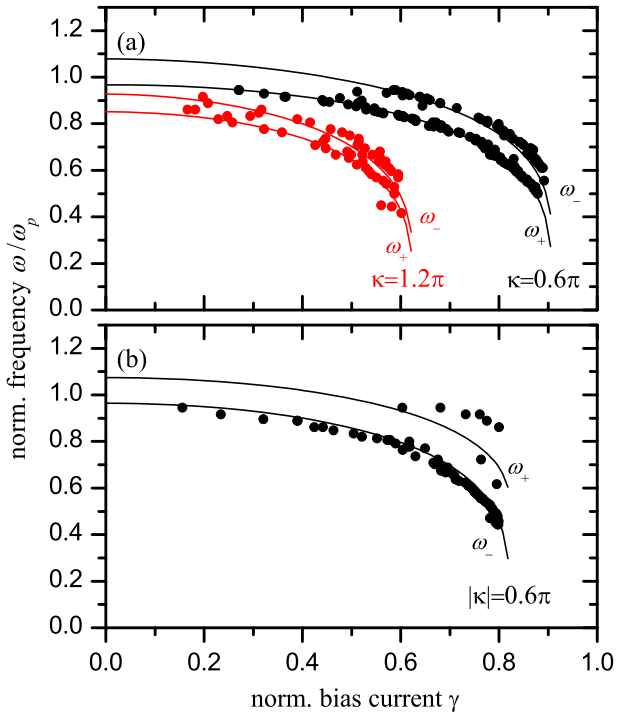

Figure 2.11: Example of experimental data (symbols) that show a splitting of the eigenfrequency of a single vortex into a two modes, ω_+ and ω_- in a molecule consisting of two fractional vortices oriented (a) ferromagnetically and (b) antiferromagnetically. The lines show the $\omega_\pm(\kappa,\gamma)$ dependences expected from the theory. Adapted from Ref. [25].

Fig. 2.10, the eigenfrequencies obtained experimentally are in good agreement with the theoretical predictions [11].

Recently our group reported the results on spectroscopy of a fractional vortex *molecule* in annular LJJs [25]. The splitting of eigenfrequencies to the in-phase and out-of-phase modes due to vortex-vortex coupling was observed. The splitting is larger for smaller vortex-vortex distance (stronger coupling). We also demonstrated that the modes split in different ways in the FM and AFM molecule in accord with numerical simulations.

2.4.2 Tunable plasmonic crystals

Author's contributions: [17]

We have seen above that in a molecule consisting of two fractional vortices the eigenfrequency ω_0 splits into $\omega_\pm$ corresponding to the in-phase and out-of-phase modes. If one takes three coupled vortices, one sees splitting into three modes with three different frequencies. One can also built a chain of N coupled fractional vortices — a *fractional vortex crystal* — and observe splitting into N modes. When $N\to\infty$, these N eigenfrequencies form a frequency band within the plasma gap. As with a single eigenfrequency, the position of this band depends on parameters of the system: distance a between vortices, topological charge of the vortex $\wp$, and the value of the bias current. Very general arguments suggest that this band gets broader for smaller a (larger coupling) and shifts to lower frequencies with $|\wp|$ and γ.

This problem was investigated numerically assuming $N=\infty$ [17]. In this case, one employs a Bloch (Floquet) theorem to find whether particular frequency belongs to the spectrum. It was shown that one can control the spectrum at the design stage by properly choosing the distance a

between the phase discontinuities as well as at *run-time*, by changing the value of $\kappa \propto I_{\rm inj}$ (in LJJ with artificial discontinuities) or the bias current γ. Also, each band configuration as a function of (a, κ, γ) in addition depends on the state of the vortex crystal. For example, it can be FM state $\uparrow\uparrow\uparrow\uparrow \ldots \uparrow\uparrow\uparrow\uparrow$, AFM state $\uparrow\downarrow\uparrow\downarrow \ldots \uparrow\downarrow\uparrow\downarrow$, polarized state $\uparrow\uparrow\uparrow\uparrow \ldots \downarrow\downarrow\downarrow\downarrow$, or something more complex, *e.g.*, $\uparrow\downarrow\downarrow\uparrow \ldots \downarrow\downarrow\downarrow\uparrow$. Transitions between such states of a crystal can be controlled by magnetic field or by bias current exceeding the rearrangement current, see Sec. 2.3.1.

2.5 Semifluxon dynamics

Author's contributions: [4, 10]

2.5.1 Zero field steps

In conventional LJJ zero field steps (ZFS) appear on the McCumber branch of the IVC, and correspond to the motion of one of more fluxons back and forth along LJJ [FD73,PW84]. Normally one can observe several steps with asymptotic voltages given by

$$V_n^{\rm ZFS} = \frac{\Phi_0 \bar{c}_0}{L} n. \tag{2.36}$$

The n-th ZFS corresponds to n fluxons moving inside the LJJ. Upon reflection at the edges each fluxon changes its polarity. Thus it moves as a fluxon from the left edge to the right one and then as antifluxon from the right edge to the left one.

It was noticed already in earlier works [Ste02] that the IVC of a 0-π LJJ also contains some steps which look similar to ZFSs. They are well visible only in the LJJ with L of the order of few λ_J and their asymptotic voltages formally corresponds to half integer n in Eq. (2.36). Therefore, these steps are often called *half-integer ZFS*.

The mechanism responsible for the appearance of half-integer ZFSs, was described by us [2,4]. In essence, the semifluxon sitting in the center of a 0-π LJJ permanently flips under the action of the bias current. This flipping can be interpreted as rearrangements $\uparrow\downarrow \rightarrow \downarrow\uparrow$ between the semifluxon and its images outside the LJJ. Such rearrangements alternate between the right and left edges of the LJJ. One flux quantum per flipping is transferred through the corresponding LJJ edge. For comparison, in classical ZFSs two flux quanta are transferred per reflection. *Assuming* that the maximum velocity of the flux transfer is equal to the Swihart velocity $\bar{c}_0$, we immediately explain twice small asymptotic voltage of half-integer ZFS. Also, since the image plays a crucial role here, it is clear that the effect will take place in a 0-π LJJ of moderate length of few λ_J.

In some sense, this steps can also be considered as classical Fiske steps induced by a non uniform magnetic field. Since in 0-π LJJ the phases at the edges are roughly differ by π, one can treat this as non-uniformly applied magnetic field. This approach, valid for relatively short 0-π LJJ, was put forward recently [NSAN06] and the expressions for "Fiske" step heights as a function of applied magnetic field were obtained. Indeed, the step at $V_1^{\rm FS} = V_{1/2}^{\rm ZFS} = \Phi_0 \bar{c}_0 / 2L$ has its maximum amplitude at zero field. Higher order steps are in fact some mixtures of ZFSs an Fiske steps: they have non-zero amplitude at $H = 0$, but this amplitude grows with $|H|$.

Half-integer ZFSs were observed by us in several experiments. First, they were observed in a 0-π LJJ with artificially created discontinuity [4]. Then, the whole series of half-integer ZFSs were also observed in SIFS 0-π LJJs and their magnetic field dependence was measured [10]. As an example, in Fig. 2.12 one can see the IVCs with half-integer ZFS and the dependence of its height on magnetic field.

The theoretical description employing a Fiske-step-like ansatz [NSAN06] is only valid for relatively short 0-π LJJ. Numerical simulations show that in a 0-π LJJ of $L = 3\lambda_J$, one may observe a fine structure of each step, corresponding to the different modes of flux motion. For example, the step with $n = 3/2$ consists of two sub-branches. The one close to the McCumber branch (lower bias) has

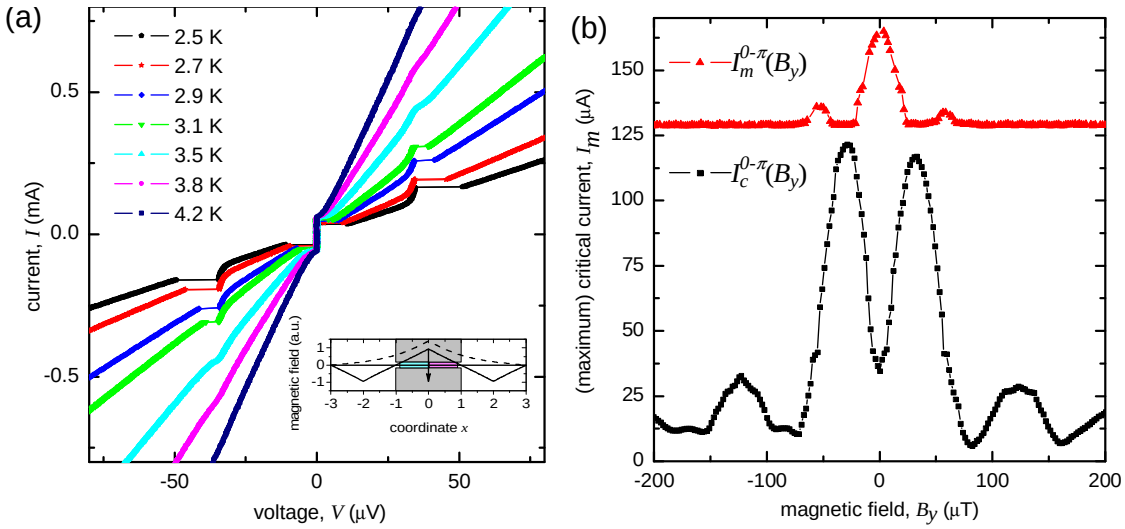

Figure 2.12: (a) A set of IVCs measured at different temperatures and at zero applied magnetic fields. One can see that as the damping decreases with temperature, a half-integer ZFS appears. (b) Measured dependence of the height $I_m(H)$ of the half-integer ZFS and of the critical current $I_c(H)$ for comparison. Adapted from Ref. [10].

higher voltage and standing-wave-like dynamics (flux motion at regular spatial intervals). The sub-branch at higher bias current has smaller voltage (larger damping) and dynamics corresponding to a bunched motion of three semifluxons.

2.5.2 Fiske steps

When a magnetic field is applied to a conventional LJJ, one can observe Fiske steps on the IVC of a LJJ. These steps are related to the resonance between the moving chain of fluxons (flux flow) and standing electromagnetic waves (cavity modes) with different mode number n. The same mechanism is also present in 0-π LJJs. The asymptotic voltage of the Fiske steps in any case is given by

$$V_n^{\mathrm{FS}} = \frac{\Phi_0 \bar{c}_0}{2L} n. \tag{2.37}$$

To obtain the n-th step height and its dependence on magnetic field and other 0-π LJJ parameters, one can use a standard approach. Assuming the phase ansatz in a form

$$\mu = hx - \omega t + \varphi(x,t), \tag{2.38}$$

where the first and the second term describe uniform advance of the phase, while the standing wave term $\varphi(x,t)$ is given by

$$\varphi(x,t) = \sum_{n=0}^{\infty} a_n \cos\frac{n\pi x}{L}\cos\omega t + \sum_{n=0}^{\infty} b_n \cos\frac{n\pi x}{L}\sin\omega t, \tag{2.39}$$

one derives expressions for the step height [NSAN06]. This approach is valid for relatively short 0-π LJJ and describes the height of ZFSs, FSs and their mixtures. Recently, the magnetic field modulation of the height of the first five Fiske step's in a SIFS 0-π LJJ of length $L = 330\,\mu\mathrm{m} \approx 0.7\lambda_J$ was measured experimentally [10] and good agreement with the theory [NSAN06] was found. An example of experimental results can be seen in Fig. 2.13

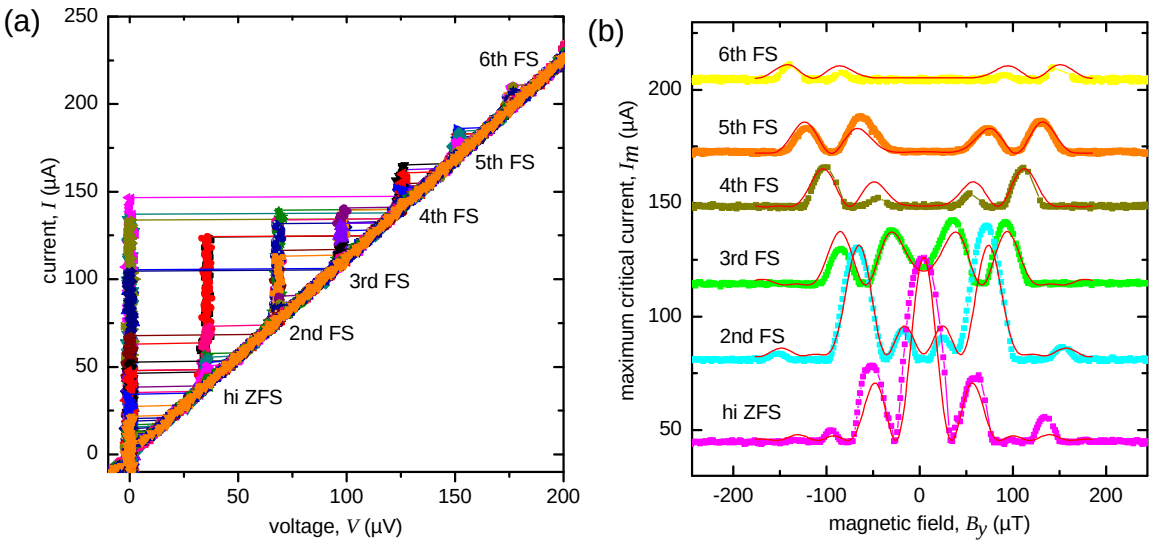

Figure 2.13: (a) A set of IVCs measured at different applied magnetic fields. (b) Measured dependence of the height $I_m(H)$ of different steps on magnetic field. Adapted from Ref. [10].

2.5.3 Shapiro steps

Although there is a number of works that present Shapiro step data on 0-π LJJs, it is quite tricky to deduce a reliable conclusion about the origin of these steps.

First, in a short (point-like), overdamped ($\beta_c = 0$) conventional 0 JJ with sinusoidal CPR one observes only integer Shapiro steps on the IVC of a JJ. The voltages of Shapiro steps are given by

$$V_n^{\mathrm{SH}} = \frac{\Phi_0}{2\pi}\omega_{\mathrm{ex}} n = \Phi_0 f_{\mathrm{ex}} n, \tag{2.40}$$

where $\omega_{\mathrm{ex}} = 2\pi f_{\mathrm{ex}}$ is the frequency of external irradiation.

If one investigates a 0-π JJ, the half-integer Shapiro steps are predicted to appear. However, half integer Shapiro steps also appear if the JJ is not short, and when β_c is finite. They also appear if the CPR is not sinusoidal. In fact, the physics of a short 0-π JJ can be reduced to an effective model of a point-like JJ having a negative second harmonic in the CPR [Min98].

Up to now, the height of Shapiro steps was measured as function of temperature in the vicinity of a 0-π crossover temperature for SFS 0-π JJ [FVHB+06]. It was shown that the half integer Shapiro steps appear in the vicinity of a 0-π crossover. It is not yet clear, whether this steps can be attributed to (a) 0-π JJ as designed or (b) to a multiple and random 0-π junctions due to roughness or (c) due to always present intrinsic second harmonic in the CPR which becomes dominant at the crossover point as the first harmonic vanishes. Moreover, in the simplest model [23] one cannot distinguish between the positive and the negative second harmonic in the CPR – only the absolute value enters in the formula for Shapiro step height. A more elaborated model taking into account damping term, seems to provide a way to make this distinction [KKK+06a, KKK+06b]

2.6 Macroscopic quantum effects

Although superconductivity and Josephson effect are essentially quantum phenomena, at the end, the dynamics of the Josephson phase is described by a classical Eq. (2.1) or (2.4). These equations are the *mean field* equations that do not take into account thermal or quantum fluctuations.

For a point-like JJ the effect of these fluctuations is investigated already for several decades [MDC87, CCD+88, WLC+03]. For example, classical equations predict that the JJ stays in the

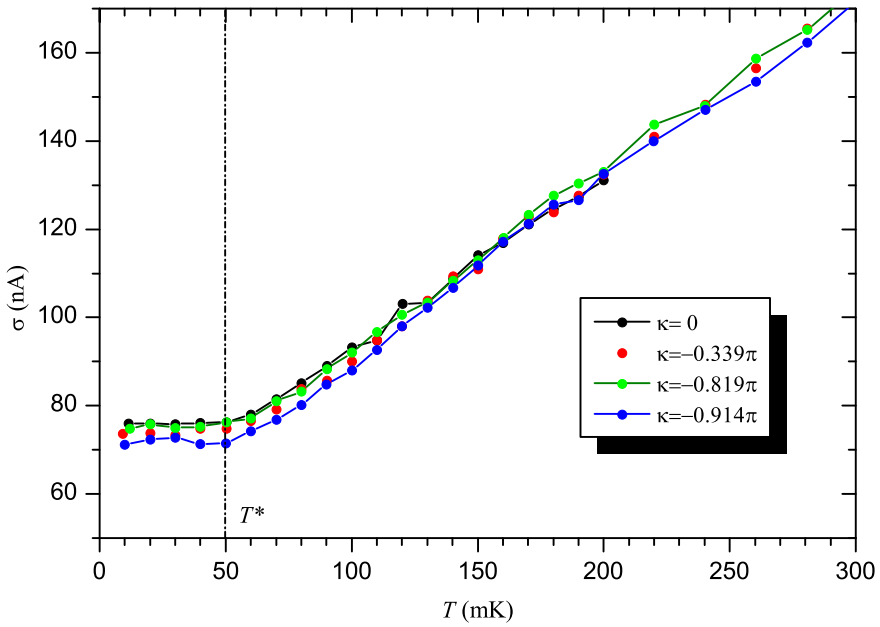

Figure 2.14: The width σ of the escape histogram as a function of temperature measured for different values of the discontinuity $\kappa \propto I_{\rm inj}$. One clearly sees the saturation of $\sigma(T)$ around $\sigma_{\rm min} \approx 75\,{\rm nA}$ for $T < T*$ — a thermal-activation-to-quantum-tunneling crossover temperature. The measurements are done in persistent mode (frozen value of $I_{\rm inj} \propto \kappa$). For this particular sample the dependence $\sigma_{\rm min}(\kappa)$ is expected to be very weak.

superconducting state if one sweeps the bias current I from zero to I_c. In reality, the JJ switches to a finite voltage state already at $I \lesssim I_c$ because of fluctuations. One can consider the escape of the phase as an escape of a particle from a pre-critically tilted washboard potential. It is clear that when the barrier ΔU, which prevents the particle from escaping, gets small at $I \to I_c$, the particle may be thermally excited over the barrier, if $\Delta U \lesssim k_B T$. In the same time, the particle may *tunnel quantum mechanically through the barrier*, if $\Delta U \lesssim \hbar\omega_p$. In experiment, one can measure the critical current of the JJ statistical number of times (say, 10000) and plot a critical current distribution histogram. Clear enough, the width of this histogram is related to the intensity of the fluctuations. If one measures the width of the histogram σ as a function of temperature T, one first observes a decrease of the width with decreasing temperature in the regime when the thermal fluctuations dominate. Below some temperature T_x the width of the histogram will not decrease any longer, indicating that we have entered a regime where the quantum fluctuations dominate in the escape process.

When this research has started, it was not quite clear whether quantum mechanics is valid for such a macroscopic variable as the Josephson phase. Nowadays the quantum mechanical features were observed in many experiments with JJs. This gives rise to a new field of macroscopic quantum effects that find immediate application, e.g., as qubits. In the area of Josephson physics, several systems such as charge qubit, flux qubit and phase qubits were implemented and tested. All of them are based on the quantum mechanical behavior of the charge, magnetic flux and Josephson phase in corresponding systems [MSS01]. Although it is commonly believed that one indeed observes quantum mechanical properties some authors point out that many experimental results (especially with microwaves applied) can be interpreted on a pure classical basis taking into account nonlinearity and thermal noise [GJC05, CZHB08, GJMCB10]. Interestingly, the observation of Rabi-oscillations at temperatures $\sim 800\,{\rm mK}$, *i.e.*, well above the classical-to-quantum crossover temperature, was reported [LLA+07].

In our group experiments on observation of macroscopic quantum effects are in progress. The

transition from thermal activation regime to MQT was observed as a saturation of the escape histogram width σ at $\sigma_{\min}$. The measurements were performed using annular LJJ equipped with injectors, which allowed to measure $\sigma(\kappa)$ curves for different fractional vortices (different κ). The biggest challenge was decreasing the injector current noise which resulted in increase of $\sigma_{\min}$ with $\kappa \propto I_{\text{inj}}$. This was finally achieved by using persistent mode in injector circuitry: after applying the desired injector current, it was frozen in a superconducting loop. In this way we were able to obtain the $\sigma_{\min}(\kappa)$ dependence that qualitatively agrees with the theory. As an example, in Fig. 2.14 one can see $\sigma(T)$ experimentally measured for different κ set using persistent mode. These results are not yet published and are subject of ongoing SFB/TRR-21. Further experiments in the quantum domain, *e.g.*, on a microwave enhanced escape, showing energy level quantization are now in progress.

2.6.1 Single semifluxon

Author's contributions: [14, 22]

As we know from Sec. 2.2.1, a single semifluxon corresponds to a ground state of the phase in a long 0-π JJ. This ground state is doubly degenerate, corresponding to semifluxon (state $\uparrow$) and antisemifluxon (state $\downarrow$). The question, which naturally arises, is: can one observe a coherent superposition of both states, i.e. something like

$$|\psi\rangle = \alpha\,|\uparrow\rangle + \beta\,|\downarrow\rangle\ ? \tag{2.41}$$

It turns out [21] that in a relatively long ($L \gtrsim \lambda_J$) 0-π LJJ the energy barrier separating two states is rather large, $\sim E_J$. Thus, the states like (2.41) are impossible and a single semifluxon is always classical. The only chance to bring a 0-π JJ in the quantum regime is to make it short. On the other hand, when it is short the flux Φ carried by "semifluxons" decreases proportionally to L^2, i.e.

$$\Phi = \Phi_0 \frac{L^2}{8\pi\lambda_J^2}, \quad L \ll \lambda_J. \tag{2.42}$$

Detailed calculations show that one can map the phase $\phi(x,t)$ dynamics to a dynamics of a point like particle moving in a periodic potential. It is equivalent to a quantum dynamics of the phase in a Josephson junction with CPR $j_s = j_c \sin(2\phi)$. The height of the potential barrier depends on the JJ length and, for typical experimental parameters, one can reach quantum regime for $L \lesssim 0.17\lambda_J$ with $T_x \sim 35\,\text{mK}$. Nevertheless, it seems that this approach is not very promising for qubit realization as one still has a rather bad two-level system — the lowest two levels are not well separated from the other states. Therefore, preparation, manipulation and readout will inevitably result in a leakage of the probability into higher states, i.e. in not exact quantum operation and decoherence.

2.6.2 Molecule of two AFM-ordered semifluxons

Author's contributions: [21]

Much better results can, in principle, be obtained using a two-semifluxon molecule in 0-π-0 LJJ. Here, the LJJ is supposed to be infinitely long, while the length of the π part (the distance between semifluxons) is equal to a. To have AFM ground state we must have $a > a_c = (\pi/2)\lambda_J$. This AFM ground state is double degenerate, being either in the $|\uparrow\downarrow\rangle$ state or in the $|\downarrow\uparrow\rangle$ state. Here the aim is to obtain the state

$$|\psi\rangle = \alpha\,|\uparrow\downarrow\rangle + \beta\,|\downarrow\uparrow\rangle\,. \tag{2.43}$$

We have developed a quantum theory of such a molecule by mapping a quantum field dynamics to the dynamics of a single particle moving in a double well potential [21]. The potential $U(B)$ is a function of collective coordinate B (dimensionless). For a exceeding a_c by few percent of λ_J,

this particle has an extremely small inertial mass $m \sim 10^{-4} m_e \lambda_J^2$, where m_e is the electron mass. Note, that since collective coordinate is dimensionless, the "mass" is measured in $kg \cdot m^2$ and can be interpreted as a moment of inertia. This mass is much smaller that of a single electron moving around the orbit with the radius λ_J. Such a small mass is hint that the quantum effects will dominate.

In fact, it was found [21] that to be in the quantum regime one has to choose the distance a very carefully. Namely, if $a = a_c + \delta a$, δa should be smaller than $0.02\lambda_J$. For $a = a_c + 0.01\lambda_J$ and typical parameters the crossover temperature was estimated to be around 100 mK — a typical value for JJ based qubits.

The requirements imposed on a are very demanding in terms of fabrication. Moreover, the energy barrier separating both states is defined by a and is not tunable. Recently we suggested to use asymmetric AFM molecules of two arbitrary fractional vortices with topological charges $(-\kappa, -\kappa + 2\pi)$ or $(-\kappa + 2\pi, -\kappa)$ in a 0-κ-2κ LJJ. By changing κ electronically, one can vary the crossover distance $a_c(\kappa)$. $a_c(\kappa)$ is a weak function of κ such as $a_c(\pi) = \pi/2$, while $a_c(0) = a_c(2\pi) \approx 1.8$. Thus, one should fabricate 0-κ-2κ LJJ with $a = 1.57 \ldots 1.8\lambda_J$ (14 % tolerance) and then electronically bring it as close to the crossover point as needed, i.e. to make the barrier as low as needed.

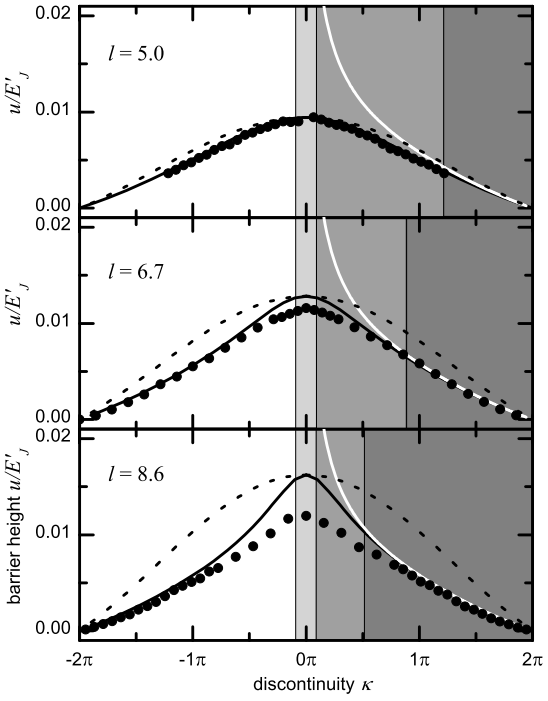

Figure 2.15: The dependence of the normalized energy barrier u/E'_J on κ for three different lengths of the annular LJJ. The symbols show experimental data (energy barrier extracted from the escape histogram). The white line shows the prediction of the theory [22], which is valid for infinite LJJ and $\kappa \ll 1$. One can see that the experimental data are indeed in accord with the theory in the region of its validity. Dashed lines show the prediction of a model of a point-like JJ with the I_c equal to the $I_c(I_{\mathrm{inj}})$ of the annular LJJ under investigation. Indeed, a short LJJ (a) can be described quite well by this simple model. Finally, the solid line shows the $u(\kappa)/E'_J$ dependence calculated numerically as the difference between energy-minimum and energy-maximum solutions. One can notice a characteristic bell-shaped bending of the curve for a longer JJ and good agreement between experimental and numerical results. Adapted from Ref. [14].

Recently, manipulation and readout of the AFM molecule states was tested in the classical domain [13] and later can be used to prepare and read out the states of the qubit. Up to now only

MQT [KI97] [22] and MQC [21] were theoretically investigated. The observation of a thermal escape of a fractional vortex was reported recently by us [14]. The thermal escape of fractional vortices was investigated in the temperature range from 4.2 K down to 300 mK and shows a non-trivial $\wp$ dependence, see Fig. 2.15. It is in good agreement with theory [22] in the limit where the theory is valid (large L and $|\wp|$) and also agrees well with numerical simulations for moderate L. We have found that for short junctions $L \lesssim 5$, the escape process takes place like in a point like JJ. For longer L a transition to vortex activation occurs. In latter case, the phase string bends over the barrier near the vortex and then pulls the rest of the phase string.

The experiments on MQT of fractional vortices are currently in progress.

2.7 Possible Applications of fractional vortices and 0-π Josephson junctions

Author's contributions: [17, 20, 23, 24]

- As described above, a single fractional vortex has an eigenfrequency, which depends, in particular, on the topological charge $\wp$ of the vortex and on the value of applied bias current γ. If we construct a molecule of two coupled vortices, the eigenfrequency will split, and the molecule will have two eigenfrequencies corresponding to in-phase and out-of-phase oscillations. The coupling strength (the distance between vortices) affects the splitting. Further, if one couples 3, 4, ..., N vortices, one gets 3, 4, ..., N eigenfrequencies. For large N these eigenmodes are very dense and form frequency band, similar to the electronic energy band in solids which and made up from single electron levels in atom. This frequency bands (and the gaps between them) depend on coupling (distance a between vortices) and can be tuned electronically during experiment by changing the value of discontinuity κ and the bias current γ. Thus, one can construct a *tunable plasmonic fractional vortex crystal*, which can be used as filter in the frequency range up to few hundreds GHz (limited by plasma frequency of JJ) [17].

- 0-π LJJs that possesses a degenerate ground state with spontaneous magnetic flux, can be used to build various devices for information storage and processing. Also, one can create huge arrays of artificial semifluxons (spins) and study collective phenomena such as formation of local/global order/disorder during the second order phase transitions [HAS+03]. This is especially interesting for frustrated systems of different geometries [KTA+05].

- One can also think about using fractional vortices or fractional vortex molecules as qubits. Theoretical estimations show that it is possible to arrive into quantum realm using a commercial 20 mK refrigerator and setup, routinely used by several groups for experiments on superconducting qubits. It is difficult to say at the moment whether a semifluxon based qubit will have any advantages over more simple systems like phase or flux qubits that may also be based on π JJs. But it will certainly look more robust than the fluxon based qubit proposed earlier since one makes manipulations between two ground states, while the fluxon is an excited state and needs additional topological protection.

- Arrays of 0-π-0-π-... segments of the lengths $a_0, a_\pi \lesssim \lambda_J$ and with $|j_c^0| \approx |j_c^\pi|$ were proposed as a system, which allows to create an effective φ JJ, *i.e.*, JJ, which has a phase drop $\phi = \pm\varphi$ in the ground state. A φ JJ is a natural generalization of a π JJ and can be used (a) to provide an arbitrary phase bias and (b) as a bistable system in the classical and the quantum domain. The physics of φ JJ was investigated in detail by us [23]. In particular, we have predicted a number of unusual properties such as: two critical currents (and two $I_c(H)$ branches), corresponding to the escape of the phase from $-\varphi$ and $+\varphi$ state; two different plasma modes; unusual field penetration (two different λ_J's for left and right edge of JJ); and, finally, two fractional Josephson vortices that are solitons of a double-sine-Gordon equation.

Recently we analyzed only one period of . . .-0-π-0-π-. . . array, i.e., simple 0-π JJ *in magnetic field*. If, similar to the original works [Min98,BK03], one derives the equation for the *spatially averaged phase* ψ one obtains the CPR of the form [24]

$$I_s = \langle I_c \rangle \left[\sin(\psi) + \Gamma_0 \sin(2\psi) + \Gamma_h h \cos(\psi) \right], \tag{2.44}$$

where $\Gamma_0 < 0$ and Γ_h are constants that depend on parameters of he sample such as $j_{c,0}$, $j_{c,\pi}$, L_0, L_π. The CPR (2.44) is remarkable. First, if $\Gamma_0 < -\frac{1}{2}$, at zero magnetic field $h = 0$ it correspond to φ JJ. Second, this CPR contains a term $\propto \cos(\psi)$, which is very unusual. Usually one has only harmonics of sine, *i.e.*, $\sin(n\psi)$. Third, the amplitude of this $\cos(\psi)$ term is proportional to the applied magnetic field, *i.e.*, it is tunable electronically during experiment. The idea is realized experimentally by us [manuscript is submitted].

- Recent experiments with arrays of 0-π-0-π-. . . segments showed that they are very sensitive to the non-uniformities of magnetic field and can be used as sensors [20]. If the field is uniform, at certain value one achieves the resonance between the period of supercurrent oscillations and the period of the array. This results in a sharp peak in the $I_c(H)$ dependence. For a non-uniform field, the periods of phase oscillation and of facets cannot not match along the whole array, so the main peak on $I_c(H)$ dependence is suppressed and rather large side peaks appear [20].

Chapter 3

Conclusions and outlook

3.1 Conclusions

As a results of theoretical, experimental and technological efforts made by our and other groups during the last decade substantial advances in technology and physics were achieved. While at the beginning of this work only 0-π JJs based on d-wave superconductors were available, at the moment the SIFS 0-π JJ technology is developed to the mature state. The supercurrent injector technology allows to create electronically tunable κ discontinuities of the phase, *i.e.*, 0-κ JJs that allow to study arbitrary fractional vortices and their molecules.

A series of theoretical papers [1–3, 6, 15–17, 21–24] and the following successful experiments [4, 5, 7–14, 18, 19] allow to claim that the classical physics of the fractional vortices is well understood. At the present moment our research is focused on the investigation of multi-vortex systems in the classical domain and on the macroscopic quantum effects.

3.2 Outlook

For nearest future the attention will be most probably focused on the exploration of quantum properties of fractional vortex matter: MQT of a fractional vortex, energy level quantization in the precritical state, coherent superposition of two-semifluxon molecule states, manipulation of states, *etc.*. Our group also proposed a qubit based on a two-semifluxon molecule. Using an the states $(-\kappa, 2\pi - \kappa)$ and $(-\kappa, 2\pi - \kappa)$ of arbitrary fractional vortices pinned at $(+\kappa, +\kappa)$ discontinuities instead of $\pm(-\pi, +\pi)$ semifluxon states, will allow to tune the energy barrier between the vortices and achieve full control of the qubit.

Acknowledgements

Many people participated, helped me in one or the other way, as well as interfered destructively or constructively in the course of this work. In particular, I would like to thanks the following persons.

- **Prof. Reinhold Kleiner** and **Prof. Dieter Kölle** for being good bosses. They not only provided me with good advices in terms of my career, project application and management, but also supported me politically and gave me enough freedom in my research. The semifluxon activity, which I started alone in 2002, grew up now into a "semifluxon group".

- I would like to thank all the guys of the "semifluxon group" for being on board now or earlier: **Tobias Gaber** (aka T2) for restless work on low-temperature setup(s) and electronics for quantum measurements; **Matthias Kemmler** for SQUID-amplifier measurements of the first in the world 0-π SIFS JJs and other projects (*e.g.*, FIB); **Kai Buckenmaier** for the first in world measurements of the eigenfrequency of fractional vortices; **Kaya Buckenmaier** for always being happy and for creating a good mood around; **Dipl. Phys. and Dipl. Bio. Judith Pfeiffer** for her choice of being a physicist ;–) and also for her fights with bad SIFS junctions; **Uta Kienzle** for being a talented student (the best drafts I ever read); **Hanna Sickinger** for being a brave student (keyword "Saleva Klettersteig")and for the measurements of the 1st φ JJs in the world; **Christian Gürlich** and **Sebastian Scharinger** for their restless LTSEM measurements; **Andreas Dewes** for being talented student who nevertheless has to learn that "the devil is hidden in details".

- All other members of the group, in particular my diploma students **Markus Beck** and **Martin Knufinke** for being motivated and autonomous. Also I thank our technology gurus **Markus Turad, Andreas Stöhr, Victor Leca** for the 2nd in the world $YBa_2Cu_3O_7$-Nb 0-π ramp zigzag junctions and **Georg Rudolf** for cutting those JJs using FIB.

- Our secretaries, **Marie-Luise Fenske** (aka ML) for a energizing "Hello, Edward" every morning and helping in many burocratic things; and **Marie-Annick Pacquier** (aka MA) for her critical attitude to things (which is not always bad), for NOT putting the gray paper into a white tray of our printer/copy-machine, and for endless discussions about everything starting from Brittany and ending by the situation on the stock market.

- **Dr. Martin Weides** for being a extremely successful Ph.D. student, pleasant collaborator, and, in particular, for the best SIFS 0, π and 0-π JJs; **Dr. Hermann Kohlstedt** and **Prof. Rainer Waser** for collaboration and support of "superconducting" activity in a "ferroelectric" institute.

- **Prof. Alexey Ustinov** for being my former Ph.D. boss, teacher, colleague and friend, and for transfer of low temperature setup "know-how" from Erlangen to Tübingen. Last, but not least, I thank him for organizing annual ski seminar, which, personally for me, is the main skiing event of the year where old friends and colleagues meet for discussions in a very informal atmosphere.

- **Dr. Hadi Susanto** for pleasant and fruitful collaboration and quick solution of several mathematical problems.
- **Prof. Alexander Buzdin** for hospitality during my visit to Bordeaux and pleasant collaboration.
- **Prof. Roman Mints** for fruitful collaboration within our GIF project and endless Soviet-time stories.
- **Dr. Konstantin Il'in** and **Prof. Michael Siegel** from University of Karlsruhe for providing our group with tons of Nb-AlO_x-Nb JJs and amazing Nb films and for pleasant collaboration in general. Special thanks to *Max Meckbach* for his high quality JJs, that Hypres still cannot provide.
- **Dr. John Kirtley** and **Dr. Chang Tsui** from IBM Research Center for their pioneering works on order parameter symmetry in cuprate superconductors that inspired our whole semifluxon activity back in 2002.
- At the end I would like to thank my father **Goldobin Boris** who, even being 3000 km away, constantly supported me morally and was interested in my research, my life far from motherland. Thanks for understanding, support and pushing me when I was too slow.

Bibliography

[AB07] J. A. Angelova and T. L. Boyadjiev. Critical relations in symmetric 0-π Josephson junctions. cond-mat/0702418, 2007.

[ADS+05] Ariando, D. Darminto, H. J. H. Smilde, V. Leca, D. H. A. Blank, H. Rogalla, and H. Hilgenkamp. Phase-sensitive order parameter symmetry test experiments utilizing $Nd_{2-x}Ce_xCuO_{4-y}$/Nb zigzag junctions. *Phys. Rev. Lett.*, 94(16):167001, 2005.

[AG84] L. G. Aslamazov and E. V. Gurovich. Pinning of solitons by Abrikosov vortices in distributed Josephson junctions. *JETP Lett.*, 40(1):746–749, 1984.

[And61] P. W. Anderson. Localized magnetic states in metals. *Phys. Rev.*, 124(1):41–53, Oct 1961.

[BBA+04] A. Bauer, J. Bentner, M. Aprili, M. L. Della Rocca, M. Reinwald, W. Wegscheider, and C. Strunk. Spontaneous supercurrent induced by ferromagnetic π junctions. *Phys. Rev. Lett.*, 92(21):217001, 2004.

[BGN+05] M. Beck, E. Goldobin, M. Neuhaus, M. Siegel, R. Kleiner, and D. Koelle. High-efficiency deterministic Josephson vortex ratchet. *Phys. Rev. Lett.*, 95(9):090603, 2005.

[BK03] A. Buzdin and A. E. Koshelev. Periodic alternating 0- and π-junction structures as realization of ϕ-Josephson junctions. *Phys. Rev. B*, 67:R220504, 2003.

[BKS77] L. N. Bulaevskiĭ, V. V. Kuziĭ, and A. A. Sobyanin. Superconducting system with weak coupling to the current in the ground state. *JETP Lett.*, 25(7):290–294, 1977. [Pis'ma Zh. Eksp. Teor. Fiz. 25, 314 (1977)].

[BKS78] L. N. Bulaevskii, V. V. Kuzii, and A. A. Sobyanin. On possibility of the spontaneous magnetic flux in a Josephson junction containing magnetic impurities. *Solid State Commun.*, 25:1053–1057, 1978.

[BLV+03] I. Bozovic, G. Logvenov, M. A. J. Verhoeven, P. Caputo, E. Goldobin, and T. H. Geballe. No mixing of superconductivity and antiferromagnetism in a high-temperature superconductor. *Nature*, 422(6934):873–875, 2003.

[BLV+04] I. Bozovic, G. Logvenov, M. A. J. Verhoeven, P. Caputo, E. Goldobin, and M. R. Beasley. Giant proximity effect in cuprate superconductors. *Phys. Rev. Lett.*, 93(15):157002, 2004.

[BMWK99] J. J. A. Baselmans, A. F. Morpurgo, B. J. Van Wees, and T. M. Klapwijk. Reversing the direction of the supercurrent in a controllable Josephson junction. *Nature (London)*, 397(6714):43–45, January 1999.

[BTKP02] Y. Blum, A. Tsukernik, M. Karpovski, and A. Palevski. Oscillations of the Superconducting Critical Current in Nb-Cu-Ni-Cu-Nb Junctions. *Phys. Rev. Lett.*, 89:187004, 2002.

[CBP+10] K Cedergren, T Bauch, H Pettersson, J R Kirtley, E Olsson, and F Lombardi. Biepitaxial $YBa_2Cu_3O_{7-x}$ 0-π Josephson junctions. *Supercond. Sci. Technol.*, 23(3):034027, 2010.

[CCD+88] John Clarke, Andrew N. Cleland, Michel H. Devoret, Daniel Esteve, and John M. Martinis. Quantum mechanics of a macroscopic variable: The phase difference of a Josephson junction. *Science*, 239(4843):992–997, 1988.

[CEM+03] B. Chesca, K. Ehrhardt, M. Mößle, R.Straub, D. Koelle, R. Kleiner, and A. Tsukada. Magnetic field dependence of the maximum supercurrent of $La_{2-x}Ce_xCuO_{4-y}$ interferometers: Evidence for a predominant $d_{x^2-y^2}$ superconducting order parameter. *Phys. Rev. Lett.*, 90:057004, 2003.

[CKB+10] K. Cedergren, J. R. Kirtley, T. Bauch, G. Rotoli, A. Troeman, H. Hilgenkamp, F. Tafuri, and F. Lombardi. Interplay between static and dynamic properties of semifluxons in $YBa_2Cu_3\mathbf{O}_{7-\delta}$ 0-π Josephson junctions. *Phys. Rev. Lett.*, 104:177003, Apr 2010.

[CSB+02] B. Chesca, R. R. Schulz, B.Goetz, C. W. Schneider, H. Hilgenkamp, and J. Mannhart. *d*-wave induced zero-field resonances in dc π-superconducting quantum interference devices. *Phys. Rev. Lett.*, 88(17):177003, Apr 2002.

[CWB+06] J.-P. Cleuziou, W. Wernsdorfer, V. Bouchiat, T. Ondarcuhu, and M. Monthioux. Carbon nanotube superconducting quantum interference device. *Nature Nanotech.*, 1(1):53–59, 2006.

[CZHB08] J. Claudon, A. Zazunov, F. W. J. Hekking, and O. Buisson. Rabi-like oscillations of an anharmonic oscillator: Classical versus quantum interpretation. *Phys. Rev. B*, 78(18):184503, 2008.

[DMEC84] Michel H. Devoret, John M. Martinis, Daniel Esteve, and John Clarke. Resonant activation from the zero-voltage state of a current-biased Josephson junction. *Phys. Rev. Lett.*, 53(13):1260–1263, Sep 1984.

[DRAK+05] M. L. Della Rocca, M. Aprili, T. Kontos, A. Gomez, and P. Spathis. Ferromagnetic 0-π junctions as classical spins. *Phys. Rev. Lett.*, 94(19):197003, 2005.

[DvDR+05] Yong-Joo Doh, Jorden A. van Dam, Aarnoud L. Roest, Erik P. A. M. Bakkers, Leo P. Kouwenhoven, and Silvano De Franceschi. Tunable supercurrent through semiconductor nanowires. *Science*, 309(5732):272–275, 2005.

[FD73] T. A. Fulton and R. C. Dynes. Single vortex propagation in Josephson tunnel junctions. *Solid State Commun.*, 12:57, 1973.

[FD74] T. A. Fulton and L. N. Dunkleberger. Lifetime of the zero-voltage state in Josephson tunnel junctions. *Phys. Rev. B*, 9(11):4760–4768, Jun 1974.

[FOB+10] A. K. Feofanov, V. A. Oboznov, V. V. Bol'ginov, J. Lisenfeld, S. Poletto, V. V. Ryazanov, A. N. Rossolenko, M. Khabipov, D. Balashov, A. B. Zorin, P. N. Dmitriev, V. P. Koshelets, and A. V. Ustinov. Implementation of superconductor/ferromagnet/superconductor π-shifters in superconducting digital and quantum circuits. *Nat. Phys.*, 6(8):593–597, 2010.

[FVHB+06] S. M. Frolov, D. J. Van Harlingen, V. V. Bolginov, V. A. Oboznov, and V. V. Ryazanov. Josephson interferometry and Shapiro step measurements of superconductor-ferromagnet-superconductor 0-π junctions. *Phys. Rev. B*, 74(2):020503(R), 2006.

[GIS07] A. Gumann, C. Iniotakis, and N. Schopohl. Geometric π Josephson junction in d-wave superconducting thin films. *Appl. Phys. Lett.*, 91(19):192502, 2007.

[GJC05] Niels Grønbech-Jensen and Matteo Cirillo. Rabi-type oscillations in a classical josephson junction. *Phys. Rev. Lett.*, 95:067001, Aug 2005.

[GJMCB10] Niels Grønbech-Jensen, Jeffrey E. Marchese, Matteo Cirillo, and James A. Blackburn. Tomography and entanglement in coupled Josephson junction qubits. *Phys. Rev. Lett.*, 105:010501, Jun 2010.

[GL86] V. B. Geshkenbeĭn and A. I. Larkin. The Josephson effect in superconductors with heavy fermions. *JETP Lett.*, 43(6):395–399, 1986.

[GLB87] V. B. Geshkenbein, A. I. Larkin, and A. Barone. Vortices with half magnetic flux quanta in "heavy-fermion" superconductors. *Phys. Rev. B*, 36:235–238, 1987.

[GMU00] E. Goldobin, B. A. Malomed, and A. V. Ustinov. Bunching of fluxons by cherenkov radiation in Josephson multilayers. *Phys. Rev. B*, 62:1414–1420, 2000.

[GNKU98] E. Goldobin, I. P. Nevirkovets, M. Yu. Kupriyanov, and A. V. Ustinov. Strong coupling effects in (Nb-Al-AlO_x)$_2$-Nb stacked Josephson junctions. *Phys. Rev. B*, 58:15078, 1998.

[Gol97] Edward Goldobin. *Coupled long Josephson junctions*. PhD thesis, Institute of Radioengineering and Electronics, Moscow, Russia, 1997. in Russian.

[GRK10] T. Golod, A. Rydh, and V. M. Krasnov. Detection of the phase shift from a single Abrikosov vortex. *Phys. Rev. Lett.*, 104(22):227003, Jun 2010.

[GSK01] E. Goldobin, A. Sterck, and D. Koelle. Josephson vortex in a ratchet potential: Theory. *Phys. Rev. E*, 63:031111, 2001.

[GU99] E. Goldobin and A. V. Ustinov. Current locking in magnetically coupled long Josephson junctions. *Phys. Rev. B*, 59:11532, 1999.

[GU00] E. Goldobin and A. V. Ustinov. Neighboring junction state effect on the fluxon motion in a Josephson stack. *Phys. Rev. B*, 62:1427–1432, 2000.

[GWTU98] E. Goldobin, A. Wallraff, N. Thyssen, and A. V. Ustinov. Cherenkov radiation in coupled long Josephson junctions. *Phys. Rev. B*, 57:130–133, 1998.

[GWU00] E. Goldobin, A. Wallraff, and A. V. Ustinov. Cherenkov radiation from fluxon in a stack of coupled long Josephson junctions. *J. Low Temp. Phys.*, 119:589, 2000.

[HAS+03] H. Hilgenkamp, Ariando, H.-J. H. Smilde, D. H. A. Blank, G. Rijnders, H. Rogalla, J. R. Kirtley, and C. C. Tsuei. Ordering and manipulation of the magnetic moments in large-scale superconducting π-loop arrays. *Nature (London)*, 422:50–53, 2003.

[HPH+02] Jian Huang, F. Pierre, Tero T. Heikkilä, Frank K. Wilhelm, and Norman O. Birge. Observation of a controllable π junction in a 3-terminal Josephson device. *Phys. Rev. B*, 66(2):020507, Jul 2002.

[Hyp] Hypres, Elmsford (NY), USA. http://www.hypres.com.

[JHvDK06] Pablo Jarillo-Herrero, Jorden A. van Dam, and Leo P. Kouwenhoven. Quantum supercurrent transistors in carbon nanotubes. *Nature (London)*, 439(7079):953–956, 2006.

[JNGR+07] H.I. Jorgensen, T. Novotny, K. Grove-Rasmussen, K. Flensberg, and P.E. Lindelof. Critical current 0-π transition in designed Josephson quantum dot junctions. *Nano Lett.*, 7(8):2441–2445, 2007.

[Jos62] B. D. Josephson. Possible new effects in superconductive tunneling. *Phys. Lett.*, 1:251–253, 1962.

[KAL+02] T. Kontos, M. Aprili, J. Lesueur, F. Genêt, B. Stephanidis, and R. Boursier. Josephson junction through a thin ferromagnetic layer: Negative coupling. *Phys. Rev. Lett.*, 89:137007, 2002.

[KAT+10] Shiro Kawabata, Yasuhiro Asano, Yukio Tanaka, Alexander A. Golubov, and Satoshi Kashiwaya. Josephson π state in a ferromagnetic insulator. *Phys. Rev. Lett.*, 104(11):117002, Mar 2010.

[KBM95] A. B. Kuklov, V. S. Boyko, and J. Malinsky. Instability in the current-biased 0-π-Josephson junction. *Phys. Rev. B*, 51(17):11965–11968, May 1995. **55**, 11878(E) (1997).

[KBM+10] M I Khabipov, D V Balashov, F Maibaum, A B Zorin, V A Oboznov, V V Bolginov, A N Rossolenko, and V V Ryazanov. A single flux quantum circuit with a ferromagnet-based josephson π-junction. *Supercond. Sci. Technol.*, 23(4):045032, 2010.

[KCK00] V. G. Kogan, J. R. Clem, and J. R. Kirtley. Josephson vortices at tricrystal boundaries. *Phys. Rev. B*, 61(13):9122–9129, April 2000.

[KDK+99] A. Yu. Kasumov, R. Deblock, M. Kociak, B. Reulet, H. Bouchiat, I. I. Khodos, Yu. B. Gorbatov, V. T. Volkov, C. Journet, and M. Burghard. Supercurrents through single-walled carbon nanotubes. *Science*, 284(5419):1508–1511, 1999.

[KI97] T. Kato and M. Imada. Vortices and quantum tunneling in current-biased 0-π-0 Josephson junctions of d-wave superconductors. *J. Phys. Soc. Jpn.*, 66(5):1445–1449, May 1997.

[KIS+12] M. Knufinke, K. Ilin, M. Siegel, D. Koelle, R. Kleiner, and E. Goldobin. Deterministic Josephson vortex ratchet with a load. *Phys. Rev. E*, 85:011122, Jan 2012.

[KKK+06a] V K Kornev, T Y Karminskaya, Y V Kislinskii, P V Komissinki, K Y Constantinian, and G A Ovsyannikov. Dynamics of underdamped Josephson junctions with nonsinusoidal current-phase relation. *J. Phys. Conf. Ser.*, 43:1105–1109, 2006.

[KKK+06b] V.K. Kornev, T.Y. Karminskaya, Y.V. Kislinskii, P.V. Komissinki, K.Y. Constantinian, and G.A. Ovsyannikov. Dynamics of underdamped Josephson junctions with non-sinusoidal current-phase relation. *Physica C*, 435:27–30, 2006.

[KM94] R. Kleiner and P. Müller. Intrinsic Josephson effects in high-T_c superconductors. *Phys. Rev. B*, 49(2):1327–1341, Jan 1994.

[KMS97] J. R. Kirtley, K. A. Moler, and D. J. Scalapino. Spontaneous flux and magnetic-interference patterns in 0-π Josephson junctions. *Phys. Rev. B*, 56:886, 1997.

[KSKM92] R. Kleiner, F. Steinmeyer, G. Kunkel, and P. Müller. Intrinsic Josephson effects in $Bi_2Sr_2CaCu_2O_8$ single crystals. *Phys. Rev. Lett.*, 68(15):2394–2397, Apr 1992.

[KTA+05] J. R. Kirtley, C. C. Tsuei, Ariando, H. J. H. Smilde, and H. Hilgenkamp. Antiferromagnetic ordering in arrays of superconducting π-rings. *Phys. Rev. B*, 72(21):214521, 2005.

[KTA+06] J. R. Kirtley, C. C. Tsuei, Ariando, C. J. M. Verwijs, S. Harkema, and H. Hilgenkamp. Angle-resolved phase-sensitive determination of the in-plane gap symmetry in $YBa_2Cu_3O_{7-\delta}$. *Nature Physics*, 2:190–194, 2006.

[KTM99] J. R. Kirtley, C. C. Tsuei, and K. A. Moler. Temperature dependence of the half-integer magnetic flux quantum. *Science*, 285:1373, 1999.

[KTR+96] J. R. Kirtley, C. C. Tsuei, M. Rupp, J. Z. Sun, L. S. Yu-Jahnes, A. Gupta, M. B. Ketchen, K. A. Moler, and M. Bhushan. Direct imaging of integer and half-integer Josephson vortices in high-T_c grain boundaries. *Phys. Rev. Lett.*, 76:1336, 1996.

[Kul66] I. O. Kulik. Magnitude of the critical Josephson tunnel current. *Sov. Phys. JETP*, 22(4):841–843, 1966. [Zh. Eksp. Teor. Fiz. **41**, 1211-1214 (1965)].

[KYG+99] V. Kurin, A. Yulin, E. Goldobin, A. Klushin, H. Kohlstedt, M. Levitchev, and N. Thyssen. Experimental investigation of Cherenkov flux-flow oscillators. *IEEE Trans. Appl. Supercond.*, 9(2):3733, 1999.

[Laz04] N. Lazarides. Critical current and fluxon dynamics in overdamped 0-π Josephson junctions. *Phys. Rev. B*, 69(21):212501, 2004.

[Lik86] K. K. Likharev. *Dynamics of Josephson Junctions and Circuits*. Gorden and Breach, Philadelphia, 1986.

[LJB+06] T. Lindström, J. Johansson, T. Bauch, E. Stepantsov, F. Lombardi, and S. A. Charlebois. Josephson dynamics of bicrystal d-wave $YBa_2Cu_3O_{7-\delta}$ dc-SQUIDs. *Phys. Rev. B*, 74:014503, Jul 2006.

[LLA+07] J. Lisenfeld, A. Lukashenko, M. Ansmann, J. M. Martinis, and A. V. Ustinov. Temperature dependence of coherent oscillations in Josephson phase qubits. *Phys. Rev. Lett.*, 99:170504, Oct 2007.

[LS91] K. K. Likharev and V. K. Semenov. RSFQ logic/memory family: a new Josephson-junction technology for sub-terahertz-clockfrequency digital systems. *IEEE Trans. Appl. Supercond.*, 1(1):3–28, March 1991.

[LTR+02] F. Lombardi, F. Tafuri, F. Ricci, F. Miletto Granozio, A. Barone, G. Testa, E. Sarnelli, J. R. Kirtley, and C. C. Tsuei. Intrinsic d-wave effects in $YBa_2Cu_3O_{7-\delta}$ grain boundary Josephson junctions. *Phys. Rev. Lett.*, 89(20):207001, November 2002.

[MDC87] John M. Martinis, Michel H. Devoret, and John Clarke. Experimental tests for the quantum behavior of a macroscopic degree of freedom: The phase difference across a Josephson junction. *Phys. Rev. B*, 35(10):4682–4698, Apr 1987.

[Min98] R. G. Mints. Self-generated flux in Josephson junction with alternating critical current density. *Phys. Rev. B*, 57(6):R3221–R3224, Feb 1998.

[MSB+99] A. Marchenkov, R. W. Simmonds, S. Backhaus, A. Loshak, J. C. Davis, and R. E. Packard. Bi-state superfluid ^{3}He weak links and the stability of Josephson π states. *Phys. Rev. Lett.*, 83(19):3860–3863, Nov 1999.

[MSS01] Yuriy Makhlin, Gerd Schön, and Alexander Shnirman. Quantum-state engineering with Josephson-junction devices. *Rev. Mod. Phys.*, 73(2):357–400, May 2001.

[MU04] B. A. Malomed and A. V. Ustinov. Creation of classical and quantum fluxons by a current dipole in a long Josephson junction. *Phys. Rev. B*, 69:064502, 2004.

[NLC02] C. Nappi, M. P. Lissitski, and R. Cristiano. Fraunhofer critical-current diffraction pattern in annular Josephson junctions with injected current. *Phys. Rev. B*, 65:132516, 2002.

[NSAN06] C. Nappi, E. Sarnelli, M. Adamo, and M. A. Navacerrada. Fiske modes in 0-π Josephson junctions. *Phys. Rev. B*, 74(14):144504, 2006.

[OAM+06] T. Ortlepp, Ariando, O. Mielke, C. J. M. Verwijs, K. F. K. Foo, H. Rogalla, F. H. Uhlmann, and H. Hilgenkamp. Flip-flopping fractional flux quanta. *Science*, 312(5779):1495–1497, 2006.

[PGRS08] E. Pallecchi, M. Gaaß, D. A. Ryndyk, and Ch. Strunk. Carbon nanotube Josephson junctions with Nb contacts. *Appl. Phys. Lett.*, 93(7):072501, 2008.

[PW84] N. F. Pedersen and D. Welner. Comparison between experiment and perturbation theory for solitons in Josephson junctions. *Phys. Rev. B*, 29(5):2551, 1984.

[ROR+01] V. V. Ryazanov, V. A. Oboznov, A. Yu. Rusanov, A. V. Veretennikov, A. A. Golubov, and J. Aarts. Coupling of two superconductors through a ferromagnet: Evidence for a π junction. *Phys. Rev. Lett.*, 86:2427, 2001.

[SAB+02] H.-J. H. Smilde, Ariando, D. H. A. Blank, G. J. Gerritsma, H. Hilgenkamp, and H. Rogalla. *d*-wave-induced Josephson current counterflow in $YBa_2Cu_3O_7$/Nb zigzag junctions. *Phys. Rev. Lett.*, 88:057004, 2002.

[SRC+10] D. Stornaiuolo, G. Rotoli, K. Cedergren, D. Born, T. Bauch, F. Lombardi, and F. Tafuri. Submicron ybacuo biepitaxial Josephson junctions: *d*-wave effects and phase dynamics. *J. Appl. Phys.*, 107(11):113901, 2010.

[Ste02] N. Stefanakis. Resonant flux motion and I–V characteristics in frustrated Josephson junctions. *Phys. Rev. B*, 66:214524, 2002.

[SYI02] A. Sugimoto, T. Yamaguchi, and I. Iguchi. Temperature dependence of half flux quantum in $YBa_2Cu_3O_{7-y}$ tricrystal thin film observed by scanning squid microscopy. *Physica C*, 367:28, 2002.

[TB97] E. Terzioglu and M. R. Beasley. Margins and yield in superconducting circuits with gain. *IEEE Trans. Appl. Supercond.*, 7(1):18–22, 1997.

[TB98] E. Terzioglu and M. R. Beasley. Complementary Josephson junction devices and circuits: A possible new approach to superconducting electronics. *IEEE Trans. Appl. Supercond.*, 8(2):48–53, 1998.

[TGB97] E. Terzioglu, D. Gupta, and M. R. Beasley. Complementary Josephson junction circuits. *IEEE Trans. Appl. Supercond.*, 7(2):3642–3645, 1997.

[TK00] C. C. Tsuei and J. R. Kirtley. Pairing symmetry in cuprate superconductors. *Rev. Mod. Phys.*, 72:969–1016, 2000.

[TK02] C. C. Tsuei and J. R. Kirtley. *d*-wave pairing symmetry in cuprate superconductors — fundamental implications and potential applications. *Physica C*, 367:1, 2002.

[TKLG03] F. Tafuri, J. R. Kirtley, F. Lombardi, and F. Miletto Granozio. Intrinsic and extrinsic *d*-wave effects in $YBa_2Cu_3O_{7-\delta}$ grain boundary Josephson junctions: Implications for π circuitry. *Phys. Rev. B*, 67:174516, May 2003.

[UGH+99] A. V. Ustinov, E. Goldobin, G. Hechtfischer, N. Thyssen, A. Wallraff, R. Kleiner, and P. Müller. Cherenkov radiation from Josephson fluxons. *Adv. Solid State Phys.*, 38:521–531, 1999.

[UK03] A. V. Ustinov and V. K. Kaplunenko. Rapid single-flux quantum logic using π-shifters. *J. Appl. Phys.*, 94(8):5405–5407, 2003.

[Ust02] A. V. Ustinov. Fluxon insertion into annular Josephson junctions. *Appl. Phys. Lett.*, 80:3153–3155, 2002.

[VGG+06] O. Vavra, S. Gazi, D. S. Golubovic, I. Vavra, J. Derer, J. Verbeeck, G. Van Tendeloo, and V. V. Moshchalkov. 0 and π phase Josephson coupling through an insulating barrier with magnetic impurities. *Phys. Rev. B*, 74(2):020502, 2006.

[VH95] D. J. Van Harlingen. Phase sensitive tests of the symmetry of the pairing state in the high-temperature superconductors — evidence for $d_{x^2-y^2}$ symmetry. *Rev. Mod. Phys.*, 67(2):515–535, Apr 1995.

[WLC+03] A. Wallraff, A. Lukashenko, C. Coqui, A. Kemp, T. Duty, and A. V. Ustinov. Switching current measurements of large area Josephson tunnel junctions. *Rev. Sci. Instr.*, 74(8):3740–3748, 2003.

[XMT95] J. H. Xu, J. H. Miller, and C. S. Ting. π-vortex state in a long 0-π-Josephson junction. *Phys. Rev. B*, 51:11958, 1995.